JCI The Journal of Clinical Investigation

Extracellular traps released by antimicrobial TH17 cells contribute to host defense

George W. Agak, … , Matteo Pellegrini, Robert L. Modlin

J Clin Invest. 2020. https://doi.org/10.1172/JCI141594.

Research In-Press Preview **Immunology**

T_H17 cell subpopulations have been defined that contribute to inflammation and homeostasis, yet the characteristics of T_H17 cells that contribute to host defense against infection are not clear. To elucidate the antimicrobial machinery of the T_H17 subset, we studied the response to *Cutibacterium acnes*, a skin commensal that is resistant to IL-26, the only known TH17 secreted protein with direct antimicrobial activity. We generated *C. acnes*-specific antimicrobial T_H17 clones ($_{AM}T_H17$) with varying antimicrobial activity against *C. acnes*, which we correlated by RNA-seq to the expression of transcripts encoding proteins that contribute to antimicrobial activity. Additionally, we validated that $_{AM}T_H17$-mediated killing of *C. acnes* as well as bacterial pathogens, was dependent on the secretion of granulysin, granzyme B, perforin and histone H2B. We found that $_{AM}T_H17$s can release fibrous structures composed of DNA decorated with the histone H2B that entangle *C. acnes* that we call T cell extracellular traps (TETs). Within acne lesions, H2B and IL-17 colocalized in $CD4^+$ T cells, in proximity to TETs in the extracellular space composed of DNA decorated with H2B. This study identifies a functionally distinct subpopulation of T_H17 cells with an ability to form TETs containing secreted antimicrobial proteins that capture and kill bacteria.

Extracellular traps released by antimicrobial T_H17 cells contribute to host defense

George W. Agak, [1*] Alice Mouton, [2] Rosane M. B. Teles, [1] Thomas Weston, [3] Marco Morselli, [4, 5] Priscila R. Andrade, [1] Matteo Pellegrini, [4, 5] & Robert L. Modlin, [1, 6]

[1]Division of Dermatology, Department of Medicine. University of California (UCLA), Los Angeles, CA-90095, USA.

[2]Department of Ecology and Evolutionary Biology. UCLA, Los Angeles, CA-90095, USA.

[3]Department of Medicine. UCLA, Los Angeles, CA-90095, USA.

[4]Department of Molecular, Cell and Developmental Biology. UCLA, Los Angeles, CA-90095, USA.

[5]Institute for Quantitative and Computational Biosciences – The Collaboratory. UCLA, Los Angeles, CA-90095, USA.

[6]Department of Microbiology, Immunology and Molecular Genetics, David Geffen School of Medicine. UCLA, Los Angeles, CA-90095, USA.

[*]Corresponding author

George W Agak:

Address correspondence to: George W Agak, UCLA Dermatology 52-121 CHS, 41833 Le Conte Avenue, Los Angeles, California, USA. Phone: 310-825-6214; Email: Gagak@mednet.ucla.edu;

Short title: Antimicrobial T_H17 cells contribute to host defense through the release of extracellular traps.

One Sentence Summary: Our study makes a significant conceptual advance in T_H17 biology and T cell-microbe interaction via the identification of a subpopulation of antimicrobial T_H17 cells that have an ability to form T cell extracellular traps and secrete a combination of antimicrobial molecules to kill both Gram-positive and Gram-negative bacteria.

Abbreviations: $_{AM}T_H17$, Antimicrobial T_H17 cells; $_{n\text{-}AM}T_H17$, Non-antimicrobial T_H17 cells; C_A, *C. acnes* strains associated with acne; C_H, *C. acnes* strains associated with healthy skin; CFU, Colony forming units; TETs, T cell extracellular traps

Key words: *C. acnes;* histones H2B; Extracellular traps; Interleukin 17.

ABSTRACT

T_H17 cell subpopulations have been defined that contribute to inflammation and homeostasis, yet the characteristics of T_H17 cells that contribute to host defense against infection are not clear. To elucidate the antimicrobial machinery of the T_H17 subset, we studied the response to *Cutibacterium acnes*, a skin commensal that is resistant to IL-26, the only known T_H17 secreted protein with direct antimicrobial activity. We generated *C. acnes*-specific antimicrobial T_H17 clones ($_{AM}T_H17$) with varying antimicrobial activity against *C. acnes*, which we correlated by RNA-seq to the expression of transcripts encoding proteins that contribute to antimicrobial activity. Additionally, we validated that $_{AM}T_H17$-mediated killing of *C. acnes* as well as bacterial pathogens, was dependent on the secretion of granulysin, granzyme B, perforin and histone H2B. We found that $_{AM}T_H17$s can release fibrous structures composed of DNA decorated with the histone H2B that entangle *C. acnes* that we call T cell extracellular traps (TETs). Within acne lesions, H2B and IL-17 colocalized in $CD4^+$ T cells, in proximity to TETs in the extracellular space composed of DNA decorated with H2B. This study identifies a functionally distinct subpopulation of T_H17 cells with an ability to form TETs containing secreted antimicrobial proteins that capture and kill bacteria.

INTRODUCTION

T cell responses represent an important component of the adaptive immune response and contribute to host defense against microbial pathogens by secreting cytokines that activate antimicrobial effector pathways and proteins that directly lyse infected targets (*1*). Classically, $CD4^+$ T cell subsets with diverse immunological functions have been distinguished based on unique cytokine secretion patterns and transcription factor profiles (*2-7*). T_H17 cells express the transcriptional factor RORγt and secrete IL-17, IL-22, and IL-26 among others. Cytokines such as TGF-β, IL-1-β, and IL-6 are involved in T_H17 cell differentiation (*8-10*), and signals from these cytokines result in the activation of the transcription factor STAT3, which directly regulates downstream genes involved in T_H17 differentiation (*11, 12*). Defective T_H17 cell responses in STAT3 deficient patients have been associated with increased susceptibility to bacterial infections, indicating that the T_H17 subset has a major role in host defense (*13-16*).

The ability of T cells to lyse infected targets cells can be accompanied by the release of antimicrobial effector molecules that kill both intracellular and extracellular bacteria. Two major mechanisms are responsible for T cell-mediated cytolytic activity. The first involves the secretion of lytic granules containing perforin and granzymes by T cells upon contact with a target, and the second involves the interaction of membrane-bound Fas ligand on T cells with Fas molecule on the target cell (*17, 18*). In addition to $CD8^+$ T cells, several *in vivo* studies have demonstrated that cytolytic CD4+ T cells can play a protective role in viral clearance, antimicrobial activity against intracellular bacteria (*19*) and elimination of tumors (*20-25*).

The identification of $CD4^+$ T mediated killing of target cells has been described within the entire heterogeneous $CD4^+$ T cell population and little is known about the extent to which $CD4^+$ T subsets are involved in $CD4^+$ T cell-mediated antimicrobial activity. In the case of the T_H17 cells, most of the work has been done in defining their role in pathologic inflammation and disease (*26,*

27). It is unclear what distinguishes inflammatory T_H17 cells elicited by pathogens from tissue resident T_H17 cells induced by commensals. Two functionally distinct populations of T_H17 cells can simultaneously reside within the gut during pathogen-induced inflammation; notably, T_H17 induced by segmented filamentous bacteria (SFB) was shown to induce non-inflammatory homeostatic T_H17 cells, whereas *Citrobacter rodentium*-induced T_H17 cells exhibited a high inflammatory cytokine profile reflecting an inflammatory effector potential (*28*). Similarly, we and others have demonstrated that *Cutibacterium acnes* is a potent inducer of IL-17 and IFN-γ in $CD4^+$ T cells, and that IL-17^+ cells are present in perifollicular infiltrates of acne lesions, indicating that T_H17 cells contribute to the pathogenesis of the disease (*8, 29*). Moreover, acne-associated (C_A) and healthy-associated (C_H) strains of *C. acnes* differentially modulate the $CD4^+$T cell responses to induce an IL-17/IFN-γ or IL-17/IL-10^+ secreting T_H17 cells respectively. However, little is known about how T_H17 cells contribute to the killing of *C. acnes* as T_H17-mediated release of the antimicrobial protein IL-26 did not reduce bacterial viability (*30*).

Here, we used RNA sequencing (RNA-seq) to determine the mechanism(s) involved in antimicrobial T_H17 cell-mediated killing of bacteria, initially studying the immune response to *C. acnes*. We generated *C. acnes*-specific antimicrobial T_H17 clones ($_{AM}T_H17$) with varying antimicrobial activity against *C. acnes*. We show that *C. acnes*-induced $_{AM}T_H17$ cells represent a subset of $CD4^+$ T_{EM} and T_{EMRA} cells. RNA-seq analysis indicate that cytotoxic gene expression in $_{AM}T_H17$ clones correlate with both protein secretion and antimicrobial activity against *C. acnes* and is dominated by a number of known antimicrobial proteins. We found that $_{AM}T_H17$ cells release histone-rich T cell extracellular traps (TETs) in conjunction with antimicrobial proteins that can entangle and kill bacteria. This suggests that $_{AM}T_H17$-mediated killing of bacteria may be a general mechanism that contributes to homeostatic regulation of bacterial colonization.

RESULTS

C. acnes-specific $_{AM}T_H17$ are highly enriched in cytotoxic genes

Besides the $CD8^+$ cytolytic T lymphocytes (CTLs), human $CD4^+$ T cells with cytolytic functions have been reported in response to viral infections (*31-34*). The $CD4^+$ T cells are able to function as CTLs *ex vivo* and can be detected following vaccinations, including against poliovirus, small pox and in response to vaccines against HIV infection (*35, 36*) and likely to play a role in host defense (*37*). Since during the propagation of long-term $CD4^+$ T cell lines in the absence of cloning, cells expressing cytotoxic and antimicrobial activity are lost after several weeks of culture (*17*), we developed a cloning strategy that involves the use of whole *C. acnes* bacteria to stimulate immune cells, and used sterile cell sorting to select for *C. acnes*-specific T_H17 cells (Fig. S1). We generated and maintained short-term cultures of stable *C. acnes* strain-specific T_H17 clones, which enabled us to recapitulate the spectrum of the biology, present in *ex vivo* T_H17 cells (*28*). The quick expansion also permitted the analysis of transcripts associated with T_H17 cells. We first compared the antimicrobial activity of supernatants derived from these clones against *C. acnes* and several bacterial strains. We identified antimicrobial T_H17 cells, hereafter termed $_{AM}T_H17$ that had antimicrobial activity against *C. acnes* and other Gram-positive and Gram-negative bacteria (Fig. 1, A and B). We also identified non-antimicrobial T_H17 clones, hereafter termed, $_{n\text{-}AM}T_H17$, that lacked antimicrobial potency (Fig. 1A). Both the $_{AM}T_H17$ and $_{n\text{-}AM}T_H17$ clones were able to secrete IL-17 upon stimulation with α-CD3/CD28 antibodies (Fig. 1C). In further comparisons of the cytokine secretion patterns of the $_{AM}T_H17$ and $_{n\text{-}AM}T_H17$ clones, we observed that the secretion of IL-17, IL-22, IL-26 and IFN-γ ($p =< 0.001$) was higher in the $_{n\text{-}AM}T_H17$ than in the $_{AM}T_H17$ clones (Fig. 1D). On the other hand, IL-10 levels were elevated within the $_{AM}T_H17$ compared to the $_{n\text{-}AM}T_H17$ clones (Fig. 1E) suggesting that the $_{AM}T_H17$ subset likely produce IL-10 in addition to other cytokines as an important regulatory molecule to dampen excessive inflammation.

We next investigated the phenotype of the T_H17 clones via flow cytometry. We analyzed 15 $_{AM}T_H17$ clones and discovered that a mean of 64% of the $_{AM}T_H17$ were enriched in the CD4-T_{EM} (T effector memory) and 34% within the T_{EMRA} subsets defined as ($CD4^+CD45RA^-CCR7^-$ and $CD4^+CD45RA^+CCR7^-$) cells respectively (Fig. 2, A and B). On the other hand, of the 5 $_{n\text{-}AM}T_H17$ clones that we analyzed, 82% were highly enriched within the CD4-T_{EM} and 15% CD4-T_{CM} ($CD4^+CD45RA^-CCR7^+$) (Fig. 2, A and C). In addition, these clones expressed transcripts associated with tissue resident memory T cells such as CXCR6, *ITGAE* (CD103), *KFL2* and *S1PR1* (Fig. S2) (*38, 39*). These data suggest that the $_{AM}T_H17$ cells are at an advanced stage of differentiation, and may have the ability to exert antimicrobial activity as they home to peripheral non-lymphoid tissues such as the skin.

$_{AM}T_H17$ cells exhibit antimicrobial activity as early as six hours

T cells are generally thought to contribute to antimicrobial activity either by releasing cytokines, which recruit and activate other cells, or by major histocompatibility complex (MHC)-restricted lysis of infected host cells (*40*). The fact that only supernatants derived from activated $_{AM}T_H17$ clones had an ability to kill *C. acnes* in *in vitro* CFU assays, suggested that these T cells were producing soluble bactericidal product(s). To further understand the mechanism(s) of T_H17 cell mediated killing, we used RNA-seq to determine differential antimicrobial gene expression in $_{AM}T_H17$ and $_{n\text{-}AM}T_H17$ clones. To this end, we took advantage of the finding that $_{AM}T_H17$ clones had varying levels of antimicrobial activity, which we termed Low, Medium and High based on the results of *C. acnes* CFU assays. Against *C. acnes* strain HL005PA2 (Fig. 2D), reductions greater than 5-log, 3-log and 1-log in CFU were observed using undiluted supernatants derived from activated High, Medium and Low $_{AM}T_H17$ clones respectively. In contrast, supernatants from activated $_{n\text{-}AM}T_H17$ clones did not exhibit antimicrobial activity against the three *C. acnes* strains that we tested (HL005PA2, HL096PA1, and HL110PA1). We next determined the killing kinetics of $_{AM}T_H17$ supernatants against *C. acnes*. As shown in (Fig. 2E), we established that

antimicrobial activity was detectable after 6h, reaching a 2-log reduction after 12h of incubation. In contrast, supernatants derived from activated $_{n\text{-}AM}T_H17$ clones lacked antimicrobial activity against *C. acnes* even after 24h incubation. Thus, in subsequent bulk RNA-seq experiments, 15 $_{AM}T_H17$ clones with varying antimicrobial activity were stimulated with α-CD3/CD28 for 6h and 12h, and as a control, we used 5 $_{n\text{-}AM}T_H17$ clones (Fig. 2D).

Identification of antimicrobial proteins of $_{AM}T_H17$ by RNA sequencing

Using the transcriptome sequencing data, we next correlated the genes that had a greater than twofold expression within $_{AM}T_H17$ over the $_{n\text{-}AM}T_H17$ with antimicrobial activity as determined by *in vitro C. acnes* CFU activity. There were 431 and 983 genes identified in the $_{AM}T_H17$ specific signatures for the 6 and 12h time point, respectively (Fig. 3, A and B). Subsequent, overlap of these genes with an antimicrobial gene list from the Gene Cards database revealed 50 and 98 common genes with significantly higher expression in $_{AM}T_H17$ compared to the $_{n\text{-}AM}T_H17$ clones at 6 and 12h time points, respectively (Fig. 3, A and B). These common genes included cytotoxic granule and antimicrobial protein genes encoding GNLY, GZMB, GZMA, PRF1, and histones H2B and H4, and were also highly enriched in the High killer $_{AM}T_H17$ as compared to the $_{n\text{-}AM}T_H17$ clones (Fig. 3, C and D, Table S1 and S2). Transcripts encoding transcription factors and receptors related to T_H17 cells such as *RORc, IL17RE* were also expressed at high levels in the $_{AM}T_H17$ clones (Fig. S3). The *GNLY* transcript had the highest mean expression in $_{AM}T_H17$ compared to the $_{n\text{-}AM}T_H17$ clones at both the 6h and 12h time-points (Fig. S3, A and B). *GNLY* is linked to the cytotoxic function of natural killer and $CD8^+$ T cells, and has a wide range of antimicrobial activity against bacteria and fungi (*18, 19*).

Cytotoxic gene expression in $_{AM}T_H17$ clones is highly correlated with protein secretion and antimicrobial activity

To assess the functional capacity of $_{AM}T_H17$, we confirmed the expression of some of the cytotoxicity-related transcripts (*GNLY, GZMB,* and *PRF1)* at the protein level following 6 and 12h *in vitro* stimulation with α-CD3/CD28 antibodies. We found that gene expression of *GNLY, GZMB, PRF1* as determined by RNA-seq had a high positive correlation with the protein secretion data (r = 0.85, 0.79 and 0.58 at 6h), and (r = 0.87, 0.64 and 0.39 at 12h), respectively (Fig. 4B and D). We then performed CFU experiments using the same supernatants that were measured using ELISA. We observed a negative correlation in *GNLY, GZMB and PRF1* gene expression and antimicrobial activity in $_{AM}T_H17$ (r = -0.89, -0.75 and -0.71 at 6h), and (r = -0.94, -0.81 and -0.63 at 12h), respectively (Fig. 4A and 4C), suggesting that the products of these genes may play an important role in $_{AM}T_H17$-mediated antimicrobial activity against a wide variety of pathogens. The correlation between *PRF1* gene correlation and perforin protein expression decreased from 6 to 12 hours. In looking at a dynamic process in which the transcripts and protein are induced and degraded with different kinetics, the correlation may vary with time (*41*). We further validated that granulysin, granzyme B and perforin are highly enriched within the $_{AM}T_H17$ and not the $_{n\text{-}AM}T_H17$ clones (Fig. S4, A and B). Therefore, our combined transcriptomics, protein analysis and antimicrobial CFU data suggest that $_{AM}T_H17$-mediated killing is a general mechanism, and just like $CD8^+$ cytolytic T lymphocytes, $_{AM}T_H17$ can secrete granulysin, granzymes, perforin and other molecules as part of their antimicrobial arsenal, and these molecules can act synergistically to target *C. acnes* and a multitude of other cutaneous pathogens.

Histones H2B contributes to $_{AM}T_H17$-mediated antimicrobial activity

RNA-seq data revealed that *GNLY* was the top gene expressed in activated $_{AM}T_H17$ compared to $_{n\text{-}AM}T_H17$. The high values of *GNLY* expression are consistent with the role of granulysin as a protein with broad-spectrum antimicrobial activity against microbial pathogens (*1*). Neutralizing the effect of granulysin using a monoclonal antibody led to a 2-log reduction but not a complete abrogation in bacteria CFU (Fig. 5A). We therefore reasoned that the $_{AM}T_H17$- mediated killing

can involve a complex of other molecules and further mined the RNA-seq data to gain a global view of additional genes highly expressed in $_{AM}T_H17$ in comparison to $_{n\text{-}AM}T_H17$ clones. We discovered that histones (HIST2H2BE, HIST4H4 and HIST1H2BG) were among the top genes that were highly expressed after stimulation of $_{AM}T_H17$. Specifically, we observed a negative correlation in *HIST2H2BE* gene expression and antimicrobial activity in $_{AM}T_H17$ (r = -0.67, at 6h), and (r = -0.77, at 12h), respectively (Fig. 5, B and D). We also found that gene expression of *HIST1H2BE* as determined by RNA-seq had a high positive correlation with the protein secretion data (r = 0.79, at 6h) and (r = 0.88, at 12h) respectively (Fig. 5, C and E). These data therefore suggested that histone H2B contributes to the $_{AM}T_H17$-mediated antimicrobial activity.

Histone proteins share essential traits of cationic antimicrobial peptides (CAMPS), and are a major antimicrobial component of neutrophil extracellular traps (NETs) (*42*). To confirm that histone H2B can negatively affect *C. acnes* growth, we used recombinant histone H2B and H4 and performed CFU assays. Indeed a 1 and 2.5-log reduction in bacterial CFU was observed when *C. acnes* was incubated with recombinant H2B and H4 respectively (Fig. 5F). Treatment of $_{AM}T_H17$ supernatants with neutralizing antibodies to histone H2B and H4 led to a 1 to -2-log reduction in bacteria CFU (Fig. S5, A). A pronounced decrease in CFU was observed against *E. coli*, and *S. aureus* (Fig. 5, G and H) treated with recombinant histone H4. Histones have been reported in the mitochondria, cytosolic granules and cell surface (*43*), and on this basis, we reasoned that the $_{AM}T_H17$ may have an ability to secrete histones upon exposure to bacteria and that these extranuclear histones can play an important role in host defense. We therefore stained the $_{AM}T_H17$ clones with α-H2B histone antibodies and DAPI and found that histone H2B could localize to the cell surface of $_{AM}T_H17$ clones (Fig. S5, B-D). To address whether $_{AM}T_H17$ secrete histone H2B, we stimulated $_{AM}T_H17$ and $_{n\text{-}AM}T_H17$ clones, harvested the supernatants and lysates and performed ELISA and western blots. Indeed, the $_{AM}T_H17$ and not the $_{n\text{-}AM}T_H17$ clones were able to secrete histones (Fig. S6). Together these data support our notion that histones can be

secreted by $_{AM}T_H17$ and that they are antimicrobial against both Gram-positive and Gram-negative bacteria.

Previous studies detected DNA in supernatants of peripheral blood mononuclear cells stimulated with phytohemagglutinin (*44, 45*). Although both human and mouse $CD4^+$ T cells could release DNA and histones, it was not determined which T cell subset was involved (*46*). We therefore next examined the ability of T_H1 and T_H2 cells to secrete histones. We demonstrate that both T_H1 and T_H2 cell lines release the signature cytokines IFN-γ and IL4, respectively upon stimulation with PMA (Fig. S6, D and E). However, both cell lines lacked the ability to secrete histones and subsequently kill *C. acnes in vitro* (Fig. S6, F). In addition, histone/DNA complex formation by these cells were undetectable by confocal microcopy (Fig. S7, A and B). These data indicate that the ability of $_{AM}T_H17$ cells to secrete histone-coated ETs as part of an antimicrobial response is specific to this T cell subpopulation.

$_{AM}T_H17$ cells release T cell extracellular traps (TETs) that entangle *C. acnes*

Based on the fact that the $_{AM}T_H17$ were viable after histone secretion, we hypothesized that the mechanism of histone secretion involves an early non-lytic extracellular trap formation that can be induced by the recognition of bacterial stimuli/products. As shown previously, the formation of extracellular traps by immune cells is an important mechanism in the innate immune response (*42, 47*). Extracellular traps are composed of chromatin coated with histones, proteases and cytosolic proteins that not only ensnare bacteria fungi and protozoans, but also provide a high concentration of antimicrobial molecules that help trap and kill bacteria and fungi (*42, 48-51*). To study the mechanism of T_H17 extracellular trap formation, we stimulated $_{AM}T_H17$ and $_{n\text{-}AM}T_H17$ clones with phorbol 12-myristate 13-acetate (PMA), α-CD3/CD28 antibodies or *C. acnes*, either in the presence or in the absence of deoxyribonuclease (DNase). Confocal staining shows histone H2B accumulated in the cytoplasm and cell surface of $_{AM}T_H17$ suggesting that traps can mediate T cell antimicrobial activity (Fig. 6 and S5, C and D). Furthermore, confocal microscopy

demonstrate that activated $_{AM}T_H17$ form TETs, that are fibrous structures composed of DNA prominently decorated with histone H2B (Fig. 6, S7 and S8). To closely visualize the TETs, we used scanning electron microscopy and revealed that $_{AM}T_H17$ are able to externalize a meshwork of extracellular traps into the extracellular space that entangle *C. acnes* (Fig. 7 and S9). We next tested the TET forming characteristics of $_{AM}T_H17$ and $_{n\text{-}AM}T_H17$ clones activated only by contact with *C. acnes*. We observed that *C. acnes* were able to induce TETs in $_{AM}T_H17$ and not the $_{n\text{-}AM}T_H17$ (Fig. 7 E and F), and that these structures could trap bacteria (Fig. 7, F). Because extracellular traps are degraded by treatment with DNase (*42*) this enzyme was added to PMA-activated $_{AM}T_H17$ followed by addition of *C. acnes*. Treatment of $_{AM}T_H17$ with DNase led to a reduction in TET formation (Fig. S9, G and H).

To explore the disease relevance of T_H17 TET formation *in vitro*, we investigated whether such extracellular structures could be detected *in vivo* in biopsy specimens from acne patients. We detected H2B and IL-17 in the inflammatory infiltrate in acne lesions but not in normal skin (Fig. S10). We further investigated the presence of extracellular traps in acne lesions using confocal microscopy labelling CD4, IL-17 and H2B as well as DAPI. We identified $CD4^+$ T cells expressing IL-17 in acne lesions (Fig. S11). The area containing $CD4^+$ $IL\text{-}17^+$ cells was selected and H2B visualized (Fig. 8). IL-17 and H2B colocalized with DNA in fibrous structures in the extracellular space proximal to the $CD4^+$ T cells indicative of extracellular trap formation. Identical structures were detected in a second acne biopsy sample (Fig. S12). The isotype controls for both samples was negative (Fig. S13). In summary, our data demonstrate that, as in several innate immune cells (*42, 47, 52-54*), $_{AM}T_H17$s can release traps composed of DNA decorated with lysine-rich histones such as H2B, providing a mechanism by which the adaptive T cell response can monitor and regulate commensals such as *C. acnes* and invading pathogens including *S. aureus*.

DISCUSSION

Most of our understanding about mechanisms of host defense against infectious disease has come from exploration of the response to pathogenic microbes. However, the vast majority of microbial encounters are those resulting from commensal and/or symbiotic relationship with the microbiota. In the case of acne vulgaris, while most humans harbor *C. acnes* on their skin, the loss of the skin microbial diversity together with the action of the innate immune response, in particular, is thought to drive the chronic inflammatory condition (*55*). The ability of *C. acnes* strains to induce differential activation of both the innate and adaptive arms of the immune response are most likely due to differences in lineage specific genetic elements among the strains (*56*). In this study, we identify $_{AM}T_H17$ cells as a population within the $CD4^+$ T_H17 subset, discovered through RNA-seq and functional analysis that utilizes a combination of antimicrobial molecules to kill *C. acnes* and other microbial pathogens. Importantly, $_{AM}T_H17$ cells have the ability to form T cell extracellular traps (TETs) *in vitro* which are also detected *in vivo* in acne lesions.

Previous studies have reported the presence of extracellular traps in neutrophils, mast cells macrophages and basophils (*42, 48, 57-59*). The ETs entrap not only Gram-positive and Gram-negative bacteria, such as *Staphylococcus aureus, Salmonella typhimurium, Streptococcus pneumoniae* and Group A streptococci, but also pathogenic fungi, such as *Candida albicans* (*42, 49, 60-62*). However, it is not known whether T cells form ETs and trap bacteria such as *C. acnes*. Notably, we observed that *C. acnes* can activate $_{AM}T_H17$ leading to the formation of T cell extracellular traps, fibrous structures composed of DNA that are prominently decorated with histone H2B, and that the TETs upon release form a meshwork in the extracellular space that have the capacity to entangle *C. acnes*. After entrapment, we visualized through scanning EM that most of the *C. acnes* were killed. However, some bacteria have developed strategies to reduce trapping and killing by repelling cationic antimicrobial peptides (CAMPs) in ETs (*63*) or by degrading the DNA backbone with a deoxyribonuclease (DNase) (*60, 62*). Treatment of TETs

with commercial DNase rendered the TETs ineffective suggesting that DNA is required for the TET structure and function. As part of the pathogenesis of acne, disruption of the pilosebaceous unit results in the entry of *C. acnes* into the dermis, which contributes to the induction of an inflammatory response. We have previously determined that IL-17$^+$ cells are present in the perifollicular infiltrate of inflamed acne lesions (*64*). Herein, we visualized TETs *in vivo* in biopsy specimens from acne lesions, observing the colocalization of fibrous structures composed of DNA and H2B in proximity to CD4$^+$ T cells expressing IL-17. We demonstrate that these TETs can contribute to an antimicrobial response against *C. acnes*, but may also contribute to inflammation.

We further characterized the full repertoire of antimicrobial molecules expressed by $_{AM}T_H17$ in our RNA-seq dataset, and identified histones as a component of $_{AM}T_H17$-mediated immunity. Histones have been reported to coat ETs of neutrophils and other innate immune cells (*42, 47*). Four core histones (H2A, H2B, H3, and H4) form an octamer, around which DNA is wrapped in nucleosomes. These histones can display biological activities different from nucleosome structures and form an important part of skin defense (*65*). Histones are hydrophobic, cationic, and can form amphipathic α-helical structures and therefore share essential traits of CAMPS. Lysine-rich histones H2A and H2B are present on the epithelial surface of the placenta, providing the placenta and fetus protection against microbial infection (*43*). In addition, histone H2A and H2B both possess the capacity to neutralize endotoxin (*66*) and in our study, we demonstrate antimicrobial activity against *E. coli*, *S. aureus* and *C. acnes.* Therefore, the observation that histone H2B gene expression highly correlated with granulysin activity in CFU assays is consistent with its antimicrobial action (*67*), but how this increased antimicrobial response is activated *in vivo* is unknown. We also observed high expression of the arginine-rich histone H4 in $_{AM}T_H17$. Histone H4 is known to mediate antimicrobial activity through the destruction of the cell membrane, and human sebocytes can release H4, which displays bactericidal activity against *S.*

aureus and *C. acnes*. The antibacterial activity of H4 is enhanced by the presence of fatty acids on the skin (*67*).

T_H17 cells are well known for their host protective role against fungal infections in barrier tissues, in particular, those caused by *Candida albicans* and in protection against extracellular bacteria (*68-71*). Our findings highlight the relevance of T_H17 immunity to the skin commensal *C. acnes* and other bacterial strains. Direct comparison of $_{AM}T_H17$ and $_{n\text{-}AM}T_H17$ clones confirmed that $_{AM}T_H17$ displayed antimicrobial activity against both Gram-positive and Gram-negative bacteria. We show that the antimicrobial activity of $_{AM}T_H17$ is associated with a rapid expression and induction of antimicrobial transcripts, the impact of which is underscored by the finding that the top most abundantly secreted antimicrobial molecules of $_{AM}T_H17$ (granulysin, histones H2B) alone accounted for nearly 50% of the antimicrobial killing. We further identified multiple antimicrobial transcripts/molecules that are functionally important to immune defense. These results suggest that the antimicrobial molecules including granulysin, granzyme B, and perforin can act synergistically as part of the antimicrobial arsenal of $_{AM}T_H17$. It therefore seems more likely that the $_{AM}T_H17$ is a functionally distinct population that serves a protective role during infection. We suggest a model where, in the case of extracellular bacteria, $_{AM}T_H17$ cells can secrete granulysin that is then attracted to the bacterial cell wall by ionic interactions mediated by positively charged arginine residues. These residues interact with the negatively charged phospholipids on the surface of the pathogen, and granulysin can then alter membrane permeability, leading to osmotic lysis by itself. We also envisage a scenario where granulysin can colocalize with the pore forming molecule perforin and act synergistically with granzyme B, histone H2B and H4 leading to osmotic lysis. Both mechanisms can allow granulysin to access the intracellular compartments in which the pathogens reside leading to bacteria killing. Additionally, the impact of other antimicrobial cytokines such as IL-26 cannot be definitively

excluded in the bacterial killing even though we did not see significant difference in IL-26 expression between the $_{AM}T_H17$ and $_{n\text{-}AM}T_H17$ clones.

ETs have been observed in diseases such as human appendicitis (*42*) sinusoids of the liver and lungs during sepsis (*72*). The evidence presented in the paper shows that those T_H17 cells that express histones make TETs and secrete a combination of molecules that have antimicrobial activity against extracellular bacteria. The TETs were detected in acne lesions, linking them to the site of disease where they could contribute to the antimicrobial response in the extracellular environment, such as in the extracellular matrix for example. Human genetic studies indicate that alterations in T_H17 cell differentiation due to STAT3 mutations, or deletion of IL-17 receptors predisposes to multiple infections, such that these mechanisms are necessary for host defense (*13, 69*). Patients with Hyper – immunoglobulin E syndrome (HIES), caused by mutations in STAT3 have few detectable T_H17 cells in peripheral blood (*69*)**;** and a failure of T_H17 CD4 cell differentiation *in vitro* (*13, 15, 73-75*). Therefore, it is not possible to study the role of TETs in STAT3 deficient T_H17 cells in humans. In addition murine and human genetic approaches point strongly to the model that IL-17RA/RC signaling in non-myeloid cells as a necessary *in vivo* effector mechanism of T_H17 cells (*76, 77*). However, these studies do not indicate whether T_H17 production of IL-17 is sufficient for host defense. It will be difficult to assess whether TETs are also necessary for host defense, as inherited mutations in HIST2H2BE have not been reported. Nevertheless, it is possible that both IL-17 and TETs contribute to host defense against extracellular bacteria. It is likely that there is redundancy in the immune response such that several antimicrobial mechanisms work additively or in synergy *in vivo* to destroy extracellular bacteria.

Although our data indicates that TETs are involved in antimicrobial responses, as are other ETs, we cannot exclude the possibility that TETs contribute to pathology. In psoriasis, neutrophil ETs

may contribute to T_H17 induction as part of the disease pathogenesis (*78*). In addition, a correlation between the presence of neutrophil ET-associated DNA and pathology has also been implicated in other diseases (42, 70), and whether this is true for *C. acnes*-induced TETs remains to be explored. A charge-mediated mechanism whereby cationic antimicrobial molecules and histones such as H2B and H4 in TETs trap negatively charged commensals such as *C. acnes* seems plausible. The fact that T_H17 cells can release traps implies that these cells can act as an important link between the innate and adaptive responses targeting efficient clearance of invading pathogens. Taken together, our data identifies a functionally distinct subpopulation of T_H17 cells with an ability to secrete antimicrobial proteins and T cell extracellular traps to capture and kill extracellular bacteria.

MATERIALS AND METHODS

Bacterial strains

C. acnes strains used in this study were obtained from Biodefense and Emerging Infections Research Resources Repository (BEI Resources) and cultured as previously described (*30*). *Staphylococcus aureus* SA113, *Pseudomonas aeruginosa* PAO1 and *Escherichia coli* DH5α were grown in Luria broth (LB) overnight at 37^0C with agitation. Overnight bacterial cultures were sub cultured and incubated until midlog was reached, which was determined to be $OD_{600} = 0.4$. Cultures were washed in sterile PBS and renormalized to $OD_{600} = 0.4$ in culture media.

PBMC isolation, stimulation and cytokine ELISAs

Peripheral blood mononuclear cells (PBMCs) were obtained from healthy donors with written informed patient consent, as approved by the University of California, Los Angeles Institutional Review Board. PBMCs were then isolated using Ficoll–Paque gradients (GE Healthcare) as previously described (*30*). Briefly, cells were cultured in T cell media (RPMI 1640, 10% heat inactivated human serum (Gemini), 2mM L-glutamine, 10U/ml penicillin and 100 µg/ml streptomycin) and stimulated with different strains of *C. acnes* at 1 multiplicity of infection (1 MOI). Levels of cytokines accumulated in culture supernatants were measured by ELISA. As a positive control for NET formation, neutrophil isolation was done using the Neutrophil Isolation Kit (Miltenyi Biotec, Auburn, CA) following manufacturer's protocol and assessed for spontaneous NET formation (incubated with RPMI medium with 2% fetal calf serum for 130 min) and for NET formation after stimulation with 20nM phorbol 12-myristate 13-acetate (PMA) for 80, 100, and 130 min as previously described (*42*).

Sterile Cell sorting, T_H17 cloning and neutrophil isolation

We developed a cloning system that uses *C. acnes* microbes and autologous monocytes as APCs. This cloning approach provides a large number of antigens and a variety of stimuli to innate

receptors to elicit polarizing cytokines for T_H17 differentiation. Briefly, PBMCs were stimulated for 16 hours with *C. acnes* strains, and cytokine secretion determined using IL-17 cytokine secretion capture assay following the manufacturer's protocol (Miltenyi). After IL-17 staining, the cells were further stained with α-CD4 antibodies (BD, clone RPA-T4) and the $CD4^+$ $IL\text{-}17^+$ cells sorted under sterile conditions using Beckton Dickinson FACS Vantage (San Jose, CA). Dead cells were excluded by DAPI staining. Sorted cells were cloned in Terasaki plates (Nunc Microwell, Sigma-Aldrich) as previously described (*30*) and maintained in T cell media supplemented with 100 U/ml IL-2 and 2ng/ml IL-23. To avoid the effect of long-term culture, T_H17 cell clones were expanded for a maximum of 13 days aliquoted and frozen, and/or used immediately for RNA-seq and subsequent functional experiments. Samples were acquired on BD Biosciences FacsScan, and analyzed using FlowJo software (V7.6). In additional experiments, human T_H1 and T_H2 cells were isolated using $CD4^+$ T cell isolation kits (Miltenyi) and cultured in the presence of IL-2 and AB serum as previously described (*79*). Levels of IFN-γ and IL-4 were determined by ELISA (R&D).

Bacterial CFU assay

C. acnes strains were grown under anaerobic conditions in Reinforced Clostridial Medium (Oxoid, Basingstroke, England) for 2 days and collected in mid-log phase. The bacteria were washed three times with the assay buffer (10 mM Tris pH 7.4, supplemented with 0.03% volume trypticase soy broth, Tris-TSB), and enumerated by applying a conversion factor of 7.5×10^7 bacteria per mL=1 OD_{600}. T_H17 culture supernatants were diluted in Tris-TSB and the CFU assays performed as previously described (*80, 81*). For the *S. aureus*, *E. coli* and *P. aeruginosa*, CFU assays; bacteria were grown as described above and resuspended in RPMI 1640. Depletion of granulysin was performed by incubating supernatants with 10ug/ml of neutralizing α-granulysin mAb (Biolegend, clone DH10) or an isotype mAb for 12 h at 4^0C. 100µl reactions

(bacteria + T_H17 supernatants or rhIL-26 or α-granulysin or α-H2B, or α-H4, Abcam) were added to 1.5-ml tubes and incubated at 37^0C with shaking for 1, 3, or 24 h after the specified incubation periods, 10-fold serial dilutions were plated on LB plates to quantify surviving CFU.

Bulk RNA-seq Library and Sequencing

Fifteen $_{AM}T_H17$ and five $_{n\text{-}AM}T_H17$ clones (control) generated from six healthy donors were stimulated with α-CD3/CD28 (BD) in T cell media. Total RNA was isolated at two time points (6 and 12h) after treatment using RLT buffer supplemented with 1% β-mecaptoethanol (QIAGEN). RNA extraction was performed on a total of forty samples according to manufacturer's instructions using RNAeasy Micro Kit (QIAGEN), including the on-column DNase treatment step. Extracted RNA was quantified with Quant-iT RiboGreen RNA Assay Kit (Invitrogen) and RNA quality was assessed using the Agilent 2200 Tapestation (RNA Assay). mRNA libraries were prepared using the Illumina TruSeq mRNALibrary Prep kit following manufacturer's protocol. Briefly, total RNA was subjected to poly-A-selection to purify messenger RNA, then fragmented and converted into double stranded cDNA. Double stranded cDNA was then end-repaired, ligated to adapters and amplified. Final libraries were quantified using PicoGreen (Invitrogen) and the quality was assessed using the Agilent 2200 Tapestation (D1000 Assay). Libraries were pooled (4 per lane) at equimolar quantities (10uM each library) and sequenced on a HiSeq 2000 sequencer (Illumina) with 50bp single-end protocol. The data discussed in this publication have been deposited in NCBI's Gene Expression Omnibus (*82*).

Bioinformatics methods

The alignment of the samples was performed using STAR 2.5.3 (*83*) using the human genome (GRCh38.90). We explored the data to check for outliers and one sample (S31) was removed from downstream analyses. For each experiment, the 19 samples were divided into groups (Low, Medium, High, and $_{n\text{-}AM}T_H17$) based on *in vitro C. acnes* CFU killing assay. We filtered reads for

low counts and remaining were normalized using TMM (trimmed mean of M-values) in the edgeR package (*84*) in R. Reads were then processed by *voomwithqualityweight* in Limma to convert into log2 counts per million (logCPM) with associated precision weights (Law et. al 2014; Ritchie et al 2015), followed by contrast comparisons. 11,995 genes and 12,040 genes were kept for contrast comparisons in the six hours and 12 hours stimulation experiments respectively. For CFU, correlation analysis, $_{AM}T_H17$ and $_{n\text{-}AM}T_H17$ (controls) clones were stimulated with α-CD3/CD28 (BD), total RNA was isolated (6 and 12h), and processed for RNA-seq. Specific $_{AM}T_H17$ gene signatures with a twofold or more expression in comparison to the $_{n\text{-}AM}T_H17$ clones were used in a correlation analysis with % antimicrobial activity determined by *in vitro C. acnes* activity. Genes with a coefficient of correlation (r) >0.5 were overlapped with a list of antimicrobial related molecules obtained from the Gene Cards database (https://www.genecards.org/). The RNAseq data have been deposited in NCBI's Gene Expression Omnibus and are accessible through GEO Series accession number GSE144852 (https://www.ncbi.nlm.nih.gov/geo/query/acc.cgi?acc=GSE144852).

Scanning Electron Microscopy

T_H17 clones were adhered on silicon wafers (Ted Pella Inc.) treated with 0.01% Poly-L-lysine (Sigma). *C. acnes* added at a 1:1 ratio were incubated for 20, 40, 60 and 90 minutes at room temperature. Samples were rinsed with warm fixative (2.5% glutaraldehyde in 0.1M sodium cacodylate buffer, pH 7.4) then incubated with fresh fixative for 1h on ice. Next, samples were rinsed 5 times (2min each) with 0.1M sodium cacodylate and then post-fixed with 2% osmium tetroxide in 0.1M sodium cacodylate for 30min on ice. Following the incubation with osmium, the samples were rinsed five times (2min each) with diH2O and then dehydrated by incubating with an ascending series of ethanol concentrations (30, 50, 70, 85, 95% 2min each). Dehydration was completed by washing the samples in 3 changes (2min each) of 100% anhydrous ethanol. Next, samples were loaded into a Tousimis Autosamdri810 critical point dryer and dried at the

critical point of CO_2 before mounting the silicon wafers onto aluminum SEM stubs with double-sided carbon tape and transferring them to an ion-beam sputter coater and coating with approximately 5nm of iridium. Finally, secondary electron images were acquired with a Zeiss Supra 40VP scanning electron microscope set to 3.5kV accelerating voltage. All reagents were purchased from Electron Microscopy Sciences (Hatfield, PA).

Cell culture, immunoperoxidase and immunofluorescence labeling

C. acnes were labeled with PKH26 (Sigma) following manufactures protocol. T_H17 clones were then treated with PMA, PKH26-labeled *C. acnes* or left untreated in T cell medium for 3h. Following stimulation, both T_H17 clones and PKH-labeled *C. acnes* and were adhered to Poly-L-lysine-coated transwells for one hour. Cells were then washed and fixed for 30 minutes with BD Cytofix/Cytoperm (BD Biosciences) before being washed again. Next cells were blocked with normal Goat Serum for 20 minutes, and immunolabeled with primary antibodies for Histone H2B (Abcam) for one hour. Following washing, cells were stained with secondary antibodies for one hour, washed and mounted with DAPI. Immunofluorescence of cell cultures was examined using a Leica-TCS-SP8 MP inverted single confocal laser-scanning microscope (Leica) at the Advanced Microscopy/Spectroscopy Laboratory Macro-Scale Imaging Laboratory (California NanoSystems Institute, UCLA). For immunoperoxidase labeling, de-identified normal skin and acne lesion specimens were obtained from the UCLA Translational Pathology Core Laboratory after signed written informed consent. Staining for histone H2B and IL-17 (Abcam) was performed using the standard streptavidin–biotin technique, using the commercial kit HRP-AEC system following manufacturer's recommendations (R&D Systems). For confocal imaging of acne tissues, immunofluorescence labeling was performed by serially incubating cryostat tissue sections with anti-human mAbs for 2 hours and washed 3 times with 1× PBS, followed by incubation with specific, fluorochrome-labeled (A488, A568, A647) goat anti–mouse immunoglobulin antibodies (Molecular Probes) for 90 minutes. Controls included staining with

isotype-matched antibodies. Nuclei were stained with DAPI (Invitrogen, Life Technologies, Thermo Fisher Scientific). Immunofluorescence of skin sections was examined using Leica-TCS-SP8 MP as described above.

Histone H2B Western blot analysis

Western blot assays were performed using supernatants and whole cell lysates from T_H17 clones. Protein concentrations were estimated by Bradford method (Thermo fisher). Briefly, lysates prepared from cells in a lysis buffer containing protease inhibitor cocktail (Roche) were separated by SDS-PAGE, transferred to PVDF membranes, and subjected to immunoblotting. Immunoblots were performed with lysates and supernatants using anti-H2B antibody (1:1000, Abcam) and b-actin (1:5000, Abcam, ab8227) as an internal control overnight.

Statistical analysis

For statistical analysis, data obtained from at least three independent experiments were performed using GraphPad Prism software version 8. If datasets were not normally distributed, a non-parametric test was used to determine significance. If more than two datasets were compared, One-way analysis of variance was used to compare variances within groups. *Post hoc* two-tailed Student's *t*-test was used for comparison between two groups. For comparisons among 3 or more groups, we used repeated measures one-way ANOVA with Greenhouse-Geisser correction, along with Tukeys's multiple comparison test, with individual variances computed for each comparison. Significant differences were considered for those probabilities $\leq 5\%$ ($P \leq 0.05$).

Study approval. This study was conducted according to the principles expressed in the Declaration of Helsinki. The study was approved by UCLA IRB (#118-00193). All donors and acne patients provided written informed consent for the collection of peripheral blood and subsequent analysis.

Author contributions

GWA conceived, designed the experiments, analyzed the data, and wrote the manuscript. GWA performed most of the experiments. RT and TW participated in confocal and scanning EM experiments. AM, PA and MM helped with RNA-seq and bioinformatics analyses. RLM and MP supervised the study, provided critical suggestions and discussions throughout the study, and revised the manuscript.

Conflict of interest

The authors state no conflict of interest

Acknowledgements.

We kindly thank the UCLA Neuroscience Genomics Core for their assistance in RNA-seq library preparation and valuable advice. Haile Salem for assistance with the flow cytometry and cell sorting and Nairy Ceja-Garcia for help with bacterial culture and CFU assays. A.M. and M.M. were supported by QCB Collaboratory Postdoctoral Fellowship (UCLA). We used computational and storage services associated with the Hoffman2 Shared Cluster provided by UCLA Institute for Digital Research and Education's Research Technology Group. Confocal laser scanning microscopy was performed at the Advanced Light Microscopy/Spectroscopy Laboratory and the Leica Microsystems Center of Excellence at the California NanoSystems Institute at UCLA with funding support from NIH Shared Instrumentation Grant S10OD025017 and NSF Major Research Instrumentation grant CHE-0722519. Flow cytometry was performed in the UCLA Jonsson Comprehensive Cancer Center (JCCC) and Center for AIDS Research Flow Cytometry Core Facility. This work was supported by NIH K01AR071479 and Burrows Wellcome CTRG 1019954 (G.W.A.)

FIGURE LEGENDS

Fig. 1. $_{AM}T_H17$ secrete T_H17-associated cytokines and are antimicrobial against *C. acnes* and other bacterial strains. (A) Observed CFU activity against *C. acnes* strain HL005PA1 after 4 h incubation with $_{AM}T_H17$ clone S26 and $_{n\text{-}AM}T_H17$ clone S35 supernatants. **(B)** Observed CFU activity against several bacterial strains after 24 h incubation with $_{AM}T_H17$ clone S26 and $_{n\text{-}AM}T_H17$ clone S35 supernatants. Data represents the mean ± SEM. n>3. ****$p<0.0001$ by repeated measures 1-way ANOVA for treatment groups compared to $_{n\text{-}AM}T_H17$ supernatants in panel D and *C. acnes* in panel E. (**C**) $_{AM}T_H17$ and $_{n\text{-}AM}T_H17$ clones were stimulated with α-CD3/CD28 for 5h and IL-17 and IFN-γ expression determined by flow cytometry. n>3. (**D-E**) Cytokine levels in $_{AM}T_H17$ clones (S26, S27, S28) and $_{n\text{-}AM}T_H17$ clones (S35, S38, S44) as determined by ELISA. Data are shown as mean ± SEM. n>3 (D and E). *$p<0.05$, **$p<0.01$, **$p<0.001$ by 2-tailed Students's *t* test.

Fig. 2. $_{AM}T_H17$ are $CD4^+$ T_{EM} and T_{EMRA} cells and demonstrate antimicrobial activity as early as six hours. (A) $_{AM}T_H17$ and $_{n\text{-}AM}T_H17$ clones were stimulated with α-CD3/CD28 and stained with antibodies to CD4, CD45RA and CCR7. The $_{AM}T_H17$ clones consisted of primarily $CD4^+CD45RA^+CCR7^-$RA (T_{EM}) and $CD4^+CD45RA^-CCR7^-$ (T_{EMRA}) whereas the $_{n\text{-}AM}T_H17$ clones consisted mainly of T_{EM} and $^+CD45RA^-CCR7^+$ (T_{CM}). Data is representative of four independent experiments using clones derived from four different donors. **(B and C)** Analysis of memory markers in $_{AM}T_H17$ clones (S5, S16, S26, S28) and $_{n\text{-}AM}T_H17$ clones (S10, S13, S35, S38) by flow cytometry (n=4). ****$p<0.0001$ by repeated measures 1-way ANOVA for T_{EM} compared to T_{CM}, T_{EMRA} and T_N. (**D**) Several $_{AM}T_H17$ and $_{n\text{-}AM}T_H17$ clones were stimulated with α-CD3/CD28 and supernatants used for CFU assays against *C. acnes* strain HL096PA1. The $_{AM}T_H17$ clones were subsequently stratified into High, Medium, and Low based on the results of the CFU assays. ****$p<0.001$ by repeated measures 1-way ANOVA, Low, Medium and High killer $_{AM}T_H17$ compared to $_{n\text{-}AM}T_H17$. (**E**) Observed antimicrobial kinetics of supernatants derived from

activated $_{AM}T_H17$ clones against several *C. acnes* strains (HL110PA1, HLA110PA3, HL043PA1, HL096PA1 HL005PA2, and ATCC6919) in CFU assays. Data are shown as mean ± SEM. n>3. ****$p<0.0001$ by repeated measures 1-way ANOVA for treatment groups compared to *C. acnes* control.

Fig. 3. Antimicrobial transcripts are highly expressed in $_{AM}T_H17$. (A and B) $_{AM}T_H17$ genes with a log_2Fold-change (FC) >2 and positively correlated with % antimicrobial activity (r>0.5) were overlapped with an antimicrobial gene list from the Gene Cards database. (**C-D**) Heatmap of the top 20 highest correlated genes with % antimicrobial activity found in the $_{AM}T_H17$ clones with Low (sky blue), Medium (yellow) and High (purple) antimicrobial activity against *C. acnes* at 6h (C) and 12h (D). Annotation for % antimicrobial activity and correlation coefficient values for each sample and gene are displayed on top (dark blue) and on the left (green). Gene expression values are displayed as Z-scores of log_{10} normalized counts.

Fig. 4. Antimicrobial gene expression in $_{AM}T_H17$ clones highly correlate with both protein secretion and antimicrobial CFU activity. (A-D) Correlation plots of *GNLY, PRF1* and *GZMB* expression in stimulated $_{AM}T_H17$ as determined by RNA-seq. Specific $_{AM}T_H17$ gene signatures with a twofold or more expression in comparison to the $_{n\text{-}AM}T_H17$ clones and that highly correlated with *C. acnes* CFU activity (A and C) and ELISA protein secretion (B and D) are shown for the 6h and 12h time points. *p* value by Student's *t* test (n=15).

Fig. 5. Histones H2B is a component of $_{AM}T_H17$ antimicrobial activity. (A) Supernatants derived from activated $_{AM}T_H17$ clone S26 were incubated with α-granulysin neutralizing antibody or control IgG for 1h prior and used in CFU assay against *C. acnes* strain HL005PA1. Data are shown as mean ± SEM. n>3. ****$p<0.0001$ by repeated measures 1-way ANOVA for treatment

groups compared to *C. acnes* control. **(B-E)** Correlation plots of HIST2H2BE gene expression in $_{AM}T_H17$ as determined in RNA-seq against CFU assays and ELISA protein secretion after 6h (B and C), and 12h (D and E). *p* value by Students t test (n=20). **(F)** Observed CFU activity against *C. acnes* strain HLA110PA3 after 4 h incubation with recombinant histones H2B, H4 and heat inactivated controls. Data are representative of 4 independent experiments. ****$p<0.0001$ by repeated measures 1-way ANOVA for treatment groups compared to *C. acnes* control.

(G) Supernatants derived from activated $_{AM}T_H17$ clone S26 were incubated with α-H2B neutralizing antibody or control IgG for 1h prior and used in CFU assay against *E. coli*. Data are representative of 3 independent experiments. ****$p<0.0001$ by repeated measures 1-way ANOVA for treatment groups compared to *E.coli* control. (**H**) *S. aureus* after 24h incubation with recombinant histone H2B and H4. Data shows average CFU from three independent experiments ****$p<0.0001$ by repeated measures 1-way ANOVA for treatment groups compared to *S. aureus* control.

Fig. 6. $_{AM}T_H17$ extracellular structures are prominently coated with Histone H2B. (A-B) $_{n\text{-}AM}T_H17$ clones S13 (A) and $_{AM}T_H17$ clone S16 (B) were stimulated with PMA for 2 hours as previously described (*42*) and incubated with PKH-labeled *C. acnes* (red) (1:1). Cells were fixed, and stained with DAPI (blue) and α-histone H2B (green). Confocal staining images are shown. White arrows indicate T cell extracellular traps and ensnared *C. acnes.* Magnification 63X.

Fig. 7. Antimicrobial T_H17 release extracellular traps that entangle *C. acnes.* Scanning electron microscopy of the interaction of $_{AM}T_H17$ and *C. acnes* at different time points. **(A)** $_{AM}T_H17$ clones were stimulated with PMA for 30 minutes. **(B and C)** PMA and *C. acnes* for 30 minutes. **(D)** α-CD3/CD28 for 30 minutes. (**E and F**) *C. acnes* 30 minutes. **(G)** PMA and *C. acnes* for 40 minutes, and **(H)** PMA, *C. acnes* and DNase for 40 minutes (*42*). Extended and released TETs can be seen attached to bacteria.

Fig. 8 Expression of T cell extracellular traps in acne lesions. (A). Confocal images of IL-17 (red), histone H2B (green), and nuclei (DAPI, blue) in acne lesions. Dashed-line boxes identify the area further studied at higher power. **(B).** Higher power magnification of the delineated regions marked in (A) showing H2B (green) and DAPI (red) only. White arrows indicate T cell extracellular traps in proximity to $CD4^{+}IL\text{-}17^{+}H2B^{+}$ triple-positive cells within acne lesions. TETs are visualized as fibrous structures containing DNA (DAPI, blue) decorated with histone H2B (green) in the extracellular space. The images are projections of confocal z stacks generated from sections of 10μm thickness. Magnification, (A) 63X with zoom 2X from lower magnification in supplemental figure S9, and (B) is zoom 4X from (A). Data is from three individual samples. Scale bar, 10μm (enlarged insets).

Supplementary figures

Fig. S1. Scheme for generation of T_H17 clones. PBMCs were isolated from normal donors and stimulated for 16 hours with either C_H or C_A associated *C. acnes* strains. Cytokine secretion was determined using IL-17 cytokine secretion capture assay. After IL-17 staining, cells were further stained with α-CD4 antibodies and the $CD4^+$ $IL\text{-}17^+$ cells sorted under sterile conditions and cloned in Terasaki plates. On day 7, *C. acnes*-specific clones were selected using T cell proliferation assays (*30*) followed by a further 6-day expansion in 24 well plates in T cell media supplemented with 100 U/ml IL-2 and 2ng/ml IL-23. On day 13, T_H17 cell clones were either frozen, and/or used immediately in subsequent functional experiments.

Fig. S2. Tissue resident memory T cell markers expressed by T_H17 clones. (**A and B**). Normalized count expression of tissue resident memory T cell genes, *CXCR6, ITGAE (CD103), KFL2* and *S1PR1* expression in $_{AM}T_H17$ compared to $_{n\text{-}AM}T_H17$ clones as determined by RNA-seq after 6h (A) and 12h (B) stimulation with α-CD3/CD28 antibodies are shown. $*p<0.05$, $**p<0.01$, $***p<0.001$ by 2-tailed Students's *t* test.

Fig. S3. $_{AM}T_H17$ antimicrobial signatures revealed by RNA-seq. (**A and B**). Normalized count expression of antimicrobial-related genes, transcriptional factors, and IL17-associated receptor genes in $_{AM}T_H17$ compared to $_{n\text{-}AM}T_H17$ clones as determined by RNA-seq after 6h (A) and 12h (B) stimulation with α-CD3/CD28 antibodies are shown. $*p<0.05$, $**p<0.01$, $***p<0.001$ by 2-tailed Students's *t* test.

Fig. S4. Secretion of antimicrobial molecules by $_{AM}T_H17$ (**A**) Flow cytometry of a representative $_{AM}T_H17$ clone S26 stimulated with α-CD3/CD28 antibodies and stained for granulysin, granzyme B and perforin. Data is representative of three independent experiments. **(B)** Secretion of cytotoxic molecules by $_{AM}T_H17$ compared to $_{n\text{-}AM}T_H17$ clones as measured by ELISA. $*p<0.05$, $**p<0.01$, $***p<0.001$ by 2-tailed Students's *t* test.

.

Fig. S5. Effects of neutralizing histone H2 and H4 on $_{AM}T_H17$ antimicrobial activity. (A) Supernatants derived from activated $_{AM}T_H17$ and $_{n\text{-}AM}T_H17$ clones were incubated with α-H2B and α-H4 neutralizing antibodies for 1h and used for CFU assay against *C. acnes* strain HL005PA1. Data is representative of three independent experiments. ****$p<0.0001$ by repeated measures 1-way ANOVA for treatment groups compared to *C. acnes* + $_{n\text{-}AM}T_H17$ control. **(B-D)** Confocal microscopy of $_{AM}T_H17$ clone S26 stimulated with PMA for 30 minutes, fixed, and stained with (B) DAPI (blue) (C) Histone H2B (green) (D) an overlay of DAPI and Histone H2B. Original magnification: ×63.

Fig. S6. Histones H2B expression in $_{AM}T_H17$ clones. Western blotting analysis of histone H2B protein expression in (**A**) supernatants and (**B**) lysates derived from activated $_{AM}T_H17$ and $_{n\text{-}AM}T_H17$ clones. (**C**) Secretion of histone H2B by $_{AM}T_H17$ compared to $_{n\text{-}AM}T_H17$ clones as measured by ELISA. ****$p<0.0001$ by repeated measures 1-way ANOVA for $_{AM}T_H17$ supernatants compared to $_{n\text{-}AM}T_H17$ Cl. S38 control. (**D and E**) Secretion of IFN-γ, IL-4 and histone H2B by T_H1 and T_H2 cell lines as measured by ELISA. ****$p<0.001$ by repeated measures 1-way ANOVA for $_{AM}T_H17$ clone compared to T_H1 cell line. (**F**) Several T_H1 and T_H2 cell lines were stimulated with PMA and supernatants used for CFU assays against *C. acnes* strain HL096PA1. Observed CFU activity is shown. ****$p<0.001$ by repeated measures 1-way ANOVA for $_{AM}T_H17$ S26 clone compared to a T_H2 cell line.

Fig. S7. Characterization of histone H2B expression on T_H1 and T_H2 cell lines. (A-B) T_H1 (A) and T_H2 cell line (B) were stimulated with PMA for 2 hours as previously described and incubated with PKH-labeled *C. acnes* (red) (1:1). Cells were fixed, stained with DAPI (blue) and

α-histone H2B isotype control antibodies (green). Confocal staining images are shown. Original magnification: x63.

Fig. S8. $_{AM}T_H17$ extracellular structures are prominently coated with Histone H2B. (A-B) $_{n\text{-}AM}T_H17$ clone S13 (A) and $_{AM}T_H17$ clone S16 (B) were stimulated with PMA for 2 hours as previously described (*42*) and incubated with PKH-labeled *C. acnes* (red) (1:1). Cells were fixed, stained with DAPI (blue) and α-histone H2B isotype control antibodies (green). Confocal staining images are shown. Original magnification: x63.

Fig. S9. $_{AM}T_H17$ release extracellular traps that entangle *C. acnes.* Scanning electron microscopy of the interaction of $_{AM}T_H17$ and $_{n\text{-}AM}T_H17$ clones with *C. acnes* at different time points. **(A-B)** $_{AM}T_H17$ clones were stimulated with PMA and *C. acnes* for 60 minutes. **(C-E)** $_{AM}T_H17$ clones stimulated with α-CD3/CD28 antibodies for 20, 30 and 60 minutes respectively. **(F)** $_{n\text{-}AM}T_H17$ clone stimulated with PMA and *C. acnes* 30 minutes. **(G)** $_{n\text{-}AM}T_H17$ clone stimulated with PMA and *C. acnes* + DNase 90 minutes. **(H)** $_{AM}T_H17$ clone stimulated with PMA and *C. acnes* + DNase 90 minutes. **(I)** neutrophil stimulated for 30 minutes with PMA and *C. acnes* positive control (*42*).

Fig. S10. Histone H2B and IL-17 expression in acne lesions. Representative section from skin biopsy specimens of normal and acne lesions stained by the immunoperoxidase method with monoclonal antibodies specific for histone H2B, IL-17 and corresponding isotype controls (n=3). Multiple histone H2B and IL-17-positive cells (brown) can be seen scattered around the dermis. Original magnification: x40.

Fig. S11. Colocalization of $CD4^+IL\text{-}17^+$ T cells in acne lesions. High power confocal images of IL-17 (red), CD4 (cyan), and nuclei (DAPI, blue) in acne lesions of two donors (D1 and D2). Merge indicate $CD4^+$T cell secreting IL-17 within acne lesions. Dashed-line boxes identify the area further studied at higher power. The images are projections of confocal z stacks generated from sections of 10µm thickness. Scale bar, 10µm (enlarged insets). Original magnification: ×63.

Fig. S12. Colocalization of $IL\text{-}17^+H2B^+$ T cells in acne lesions. (A) Confocal images of IL-17 (red), histone H2B (green), and nuclei (DAPI, blue) in acne lesions. Dashed-line boxes identify the area further studied at higher power. **(B).** Higher power magnification of the delineated regions marked in (A) showing H2B (green) and DAPI (blue) only. White arrows indicate T cell extracellular traps in proximity to $CD4^+IL\text{-}17^+H2B^+$ triple-positive cells within acne lesions. TETs are visualized as fibrous structures containing DNA (DAPI, blue) decorated with histone H2B (green) in the extracellular space. The images are projections of confocal z stacks generated from sections of 10µm thickness. Magnification, (A) 63X with zoom 2X from lower magnification in supplemental figure S11, and (B) is zoom 4X from (A). Data is from three individual samples. Scale bar, 10µm (enlarged insets).

Fig. S13. Colocalization of $IL\text{-}17^+H2B^+$ T cells in acne lesions. (A) High power confocal images of acne lesions from donor D1 labeled with isotype control antibodies; CD4 isotype (mIgG1; cyan), IL-17 isotype (mIgG2b; red), histone H2B isotype (rabbit IgG; green), and nuclei (DAPI, blue). (B) High power confocal images of acne lesions from donor D2 labeled with isotype control antibodies; CD4 isotype (mIgG1; cyan), IL-17 isotype (mIgG2b; red), histone H2B isotype (rabbit IgG; green), and nuclei (DAPI, blue). The images are projections of confocal z stacks generated from sections of 10µm thickness. Scale bar, 10µm (enlarged insets). Original magnification: ×63.

Table S1. Common genes expressed in the $_{AM}T_H17$ clones after 6h stimulation. Specific $_{AM}T_H17$ gene signatures with a twofold or more expression in comparison to the $_{n\text{-}AM}T_H17$ clones and that highly correlated with CFU activity were overlapped with an antimicrobial gene list from the Gene Cards database. 30 common genes at 6h time point are listed. The top 20 genes are listed in figure 3.

Table S2. Common genes expressed in the $_{AM}T_H17$ clones after 12h stimulation. Specific $_{AM}T_H17$ gene signatures with a twofold or more expression in comparison to the $_{N\ n\text{-}AM}T_H17$ clones and that highly correlated with CFU activity were overlapped with an antimicrobial gene list from the Gene Cards database. 78 common genes at the 12h time point are listed. The top 20 genes are listed in figure 3.

REFERENCES

1. Ernst WA, Thoma-Uszynski S, Teitelbaum R, Ko C, Hanson DA, Clayberger C, et al. Granulysin, a T cell product, kills bacteria by altering membrane permeability. *J Immunol.* 2000;165(12):7102-8.
2. Hirahara K, Poholek A, Vahedi G, Laurence A, Kanno Y, Milner JD, et al. Mechanisms underlying helper T-cell plasticity: implications for immune-mediated disease. *J Allergy Clin Immunol.* 2013;131(5):1276-87.
3. Nakayamada S, Takahashi H, Kanno Y, and O'Shea JJ. Helper T cell diversity and plasticity. *Curr Opin Immunol.* 2012;24(3):297-302.
4. Crotty S. T follicular helper cell differentiation, function, and roles in disease. *Immunity.* 2014;41(4):529-42.
5. Crotty S. A brief history of T cell help to B cells. *Nat Rev Immunol.* 2015;15(3):185-9.
6. Korn T, Bettelli E, Oukka M, and Kuchroo VK. IL-17 and Th17 Cells. *Annual review of immunology.* 2009;27:485-517.
7. Vignali DA, Collison LW, and Workman CJ. How regulatory T cells work. *Nature reviews Immunology.* 2008;8(7):523-32.
8. Agak GW, Qin M, Nobe J, Kim MH, Krutzik SR, Tristan GR, et al. Propionibacterium acnes Induces an IL-17 Response in Acne Vulgaris that Is Regulated by Vitamin A and Vitamin D. *J Invest Dermatol.* 2014;134(2):366-73.
9. Harrington LE, Hatton RD, Mangan PR, Turner H, Murphy TL, Murphy KM, et al. Interleukin 17-producing CD4+ effector T cells develop via a lineage distinct from the T helper type 1 and 2 lineages. *Nature immunology.* 2005;6(11):1123-32.
10. Zhou L, Ivanov, II, Spolski R, Min R, Shenderov K, Egawa T, et al. IL-6 programs T(H)-17 cell differentiation by promoting sequential engagement of the IL-21 and IL-23 pathways. *Nature immunology.* 2007;8(9):967-74.
11. Ivanov, II, McKenzie BS, Zhou L, Tadokoro CE, Lepelley A, Lafaille JJ, et al. The orphan nuclear receptor RORgammat directs the differentiation program of proinflammatory IL-17+ T helper cells. *Cell.* 2006;126(6):1121-33.
12. Durant L, Watford WT, Ramos HL, Laurence A, Vahedi G, Wei L, et al. Diverse targets of the transcription factor STAT3 contribute to T cell pathogenicity and homeostasis. *Immunity.* 2010;32(5):605-15.
13. Ma CS, Chew GY, Simpson N, Priyadarshi A, Wong M, Grimbacher B, et al. Deficiency of Th17 cells in hyper IgE syndrome due to mutations in STAT3. *J Exp Med.* 2008;205(7):1551-7.
14. Meller S, Di Domizio J, Voo KS, Friedrich HC, Chamilos G, Ganguly D, et al. T(H)17 cells promote microbial killing and innate immune sensing of DNA via interleukin 26. *Nat Immunol.* 2015;16(9):970-9.
15. de Beaucoudrey L, Puel A, Filipe-Santos O, Cobat A, Ghandil P, Chrabieh M, et al. Mutations in STAT3 and IL12RB1 impair the development of human IL-17-producing T cells. *J Exp Med.* 2008;205(7):1543-50.
16. Basu R, Hatton RD, and Weaver CT. The Th17 family: flexibility follows function. *Immunol Rev.* 2013;252(1):89-103.
17. Williams NS, and Engelhard VH. Identification of a population of CD4+ CTL that utilizes a perforin- rather than a Fas ligand-dependent cytotoxic mechanism. *J Immunol.* 1996;156(1):153-9.
18. Stenger S, Hanson DA, Teitelbaum R, Dewan P, Niazi KR, Froelich CJ, et al. An antimicrobial activity of cytolytic T cells mediated by granulysin. *Science.* 1998;282(5386):121-5.
19. Ochoa MT, Stenger S, Sieling PA, Thoma-Uszynski S, Sabet S, Cho S, et al. T-cell release of granulysin contributes to host defense in leprosy. *Nat Med.* 2001;7(2):174-9.

20. Wilkinson TM, Li CK, Chui CS, Huang AK, Perkins M, Liebner JC, et al. Preexisting influenza-specific CD4+ T cells correlate with disease protection against influenza challenge in humans. *Nat Med.* 2012;18(2):274-80.
21. Yasukawa M, Inatsuki A, and Kobayashi Y. Differential in vitro activation of CD4+CD8- and CD8+CD4- herpes simplex virus-specific human cytotoxic T cells. *J Immunol.* 1989;143(6):2051-7.
22. Eichelberger M, Allan W, Zijlstra M, Jaenisch R, and Doherty PC. Clearance of influenza virus respiratory infection in mice lacking class I major histocompatibility complex-restricted CD8+ T cells. *J Exp Med.* 1991;174(4):875-80.
23. Muller D, Koller BH, Whitton JL, LaPan KE, Brigman KK, and Frelinger JA. LCMV-specific, class II-restricted cytotoxic T cells in beta 2-microglobulin-deficient mice. *Science.* 1992;255(5051):1576-8.
24. Frey AB. Rat mammary adenocarcinoma 13762 expressing IFN-gamma elicits antitumor CD4+ MHC class II-restricted T cells that are cytolytic in vitro and tumoricidal in vivo. *J Immunol.* 1995;154(9):4613-22.
25. Verma S, Weiskopf D, Gupta A, McDonald B, Peters B, Sette A, et al. Cytomegalovirus-Specific CD4 T Cells Are Cytolytic and Mediate Vaccine Protection. *J Virol.* 2016;90(2):650-8.
26. Bunte K, and Beikler T. Th17 Cells and the IL-23/IL-17 Axis in the Pathogenesis of Periodontitis and Immune-Mediated Inflammatory Diseases. *Int J Mol Sci.* 2019;20(14).
27. Kryczek I, Zhao E, Liu Y, Wang Y, Vatan L, Szeliga W, et al. Human TH17 cells are long-lived effector memory cells. *Sci Transl Med.* 2011;3(104):104ra0.
28. Omenetti S, Bussi C, Metidji A, Iseppon A, Lee S, Tolaini M, et al. The Intestine Harbors Functionally Distinct Homeostatic Tissue-Resident and Inflammatory Th17 Cells. *Immunity.* 2019;51(1):77-89.e6.
29. Kistowska M, Meier B, Proust T, Feldmeyer L, Cozzio A, Kuendig T, et al. Propionibacterium acnes promotes Th17 and Th17/Th1 responses in acne patients. *J Invest Dermatol.* 2015;135(1):110-8.
30. Agak GW, Kao S, Ouyang K, Qin M, Moon D, Butt A, et al. Phenotype and Antimicrobial Activity of Th17 Cells Induced by Propionibacterium acnes Strains Associated with Healthy and Acne Skin. *J Invest Dermatol.* 2018;138(2):316-24.
31. Juno JA, van Bockel D, Kent SJ, Kelleher AD, Zaunders JJ, and Munier CM. Cytotoxic CD4 T Cells-Friend or Foe during Viral Infection? *Front Immunol.* 2017;8:19.
32. Appay V, Zaunders JJ, Papagno L, Sutton J, Jaramillo A, Waters A, et al. Characterization of CD4(+) CTLs ex vivo. *J Immunol.* 2002;168(11):5954-8.
33. Zaunders JJ, Dyer WB, Wang B, Munier ML, Miranda-Saksena M, Newton R, et al. Identification of circulating antigen-specific CD4+ T lymphocytes with a CCR5+, cytotoxic phenotype in an HIV-1 long-term nonprogressor and in CMV infection. *Blood.* 2004;103(6):2238-47.
34. Norris PJ, Moffett HF, Yang OO, Kaufmann DE, Clark MJ, Addo MM, et al. Beyond help: direct effector functions of human immunodeficiency virus type 1-specific CD4(+) T cells. *J Virol.* 2004;78(16):8844-51.
35. van Leeuwen EM, Remmerswaal EB, Vossen MT, Rowshani AT, Wertheim-van Dillen PM, van Lier RA, et al. Emergence of a CD4+CD28- granzyme B+, cytomegalovirus-specific T cell subset after recovery of primary cytomegalovirus infection. *J Immunol.* 2004;173(3):1834-41.
36. Brown DM. Cytolytic CD4 cells: Direct mediators in infectious disease and malignancy. *Cell Immunol.* 2010;262(2):89-95.
37. Patil VS, Madrigal A, Schmiedel BJ, Clarke J, O'Rourke P, de Silva AD, et al. Precursors of human CD4(+) cytotoxic T lymphocytes identified by single-cell transcriptome analysis. *Sci Immunol.* 2018;3(19).

38. Clark RA. Resident memory T cells in human health and disease. *Science translational medicine.* 2015;7(269):269rv1.
39. Liu Y, Ma C, and Zhang N. Tissue-Specific Control of Tissue-Resident Memory T Cells. *Crit Rev Immunol.* 2018;38(2):79-103.
40. Levitz SM, Mathews HL, and Murphy JW. Direct antimicrobial activity of T cells. *Immunol Today.* 1995;16(8):387-91.
41. Vogel C, and Marcotte EM. Insights into the regulation of protein abundance from proteomic and transcriptomic analyses. *Nat Rev Genet.* 2012;13(4):227-32.
42. Brinkmann V, Reichard U, Goosmann C, Fauler B, Uhlemann Y, Weiss DS, et al. Neutrophil extracellular traps kill bacteria. *Science.* 2004;303(5663):1532-5.
43. Kim HS, Cho JH, Park HW, Yoon H, Kim MS, and Kim SC. Endotoxin-neutralizing antimicrobial proteins of the human placenta. *J Immunol.* 2002;168(5):2356-64.
44. Rogers JC, Boldt D, Kornfeld S, Skinner A, and Valeri CR. Excretion of deoxyribonucleic acid by lymphocytes stimulated with phytohemagglutinin or antigen. *Proceedings of the National Academy of Sciences of the United States of America.* 1972;69(7):1685-9.
45. Rogers JC. Identification of an intracellular precursor to DNA excreted by human lymphocytes. *Proceedings of the National Academy of Sciences of the United States of America.* 1976;73(9):3211-5.
46. Costanza M, Poliani PL, Portararo P, Cappetti B, Musio S, Pagani F, et al. DNA threads released by activated CD4(+) T lymphocytes provide autocrine costimulation. *Proceedings of the National Academy of Sciences of the United States of America.* 2019;116(18):8985-94.
47. Daniel C, Leppkes M, Munoz LE, Schley G, Schett G, and Herrmann M. Extracellular DNA traps in inflammation, injury and healing. *Nature reviews Nephrology.* 2019.
48. Guimaraes-Costa AB, Nascimento MT, Froment GS, Soares RP, Morgado FN, Conceicao-Silva F, et al. Leishmania amazonensis promastigotes induce and are killed by neutrophil extracellular traps. *Proc Natl Acad Sci U S A.* 2009;106(16):6748-53.
49. Urban CF, Reichard U, Brinkmann V, and Zychlinsky A. Neutrophil extracellular traps capture and kill Candida albicans yeast and hyphal forms. *Cell Microbiol.* 2006;8(4):668-76.
50. Urban C, and Zychlinsky A. Netting bacteria in sepsis. *Nat Med.* 2007;13(4):403-4.
51. Fuchs TA, Abed U, Goosmann C, Hurwitz R, Schulze I, Wahn V, et al. Novel cell death program leads to neutrophil extracellular traps. *J Cell Biol.* 2007;176(2):231-41.
52. von Kockritz-Blickwede M, Goldmann O, Thulin P, Heinemann K, Norrby-Teglund A, Rohde M, et al. Phagocytosis-independent antimicrobial activity of mast cells by means of extracellular trap formation. *Blood.* 2008;111(6):3070-80.
53. Yousefi S, Gold JA, Andina N, Lee JJ, Kelly AM, Kozlowski E, et al. Catapult-like release of mitochondrial DNA by eosinophils contributes to antibacterial defense. *Nat Med.* 2008;14(9):949-53.
54. Ueki S, Konno Y, Takeda M, Moritoki Y, Hirokawa M, Matsuwaki Y, et al. Eosinophil extracellular trap cell death-derived DNA traps: Their presence in secretions and functional attributes. *J Allergy Clin Immunol.* 2016;137(1):258-67.
55. Dreno B, Pecastaings S, Corvec S, Veraldi S, Khammari A, and Roques C. Cutibacterium acnes (Propionibacterium acnes) and acne vulgaris: a brief look at the latest updates. *J Eur Acad Dermatol Venereol.* 2018;32 Suppl 2:5-14.
56. Tomida S, Nguyen L, Chiu BH, Liu J, Sodergren E, Weinstock GM, et al. Pan-genome and comparative genome analyses of propionibacterium acnes reveal its genomic diversity in the healthy and diseased human skin microbiome. *mBio.* 2013;4(3):e00003-13.

57. Wong KW, and Jacobs WR, Jr. Mycobacterium tuberculosis exploits human interferon gamma to stimulate macrophage extracellular trap formation and necrosis. *J Infect Dis.* 2013;208(1):109-19.
58. Mollerherm H, von Kockritz-Blickwede M, and Branitzki-Heinemann K. Antimicrobial Activity of Mast Cells: Role and Relevance of Extracellular DNA Traps. *Front Immunol.* 2016;7:265.
59. Yousefi S, Morshed M, Amini P, Stojkov D, Simon D, von Gunten S, et al. Basophils exhibit antibacterial activity through extracellular trap formation. *Allergy.* 2015;70(9):1184-8.
60. Beiter K, Wartha F, Albiger B, Normark S, Zychlinsky A, and Henriques-Normark B. An endonuclease allows Streptococcus pneumoniae to escape from neutrophil extracellular traps. *Curr Biol.* 2006;16(4):401-7.
61. Wartha F, and Henriques-Normark B. ETosis: a novel cell death pathway. *Sci Signal.* 2008;1(21):pe25.
62. Buchanan JT, Simpson AJ, Aziz RK, Liu GY, Kristian SA, Kotb M, et al. DNase expression allows the pathogen group A Streptococcus to escape killing in neutrophil extracellular traps. *Curr Biol.* 2006;16(4):396-400.
63. Wartha F, Beiter K, Albiger B, Fernebro J, Zychlinsky A, Normark S, et al. Capsule and D-alanylated lipoteichoic acids protect Streptococcus pneumoniae against neutrophil extracellular traps. *Cell Microbiol.* 2007;9(5):1162-71.
64. Agak GW, Qin M, Nobe J, Kim MH, Krutzik SR, Tristan GR, et al. Propionibacterium acnes Induces an IL-17 Response in Acne Vulgaris that Is Regulated by Vitamin A and Vitamin D. *The Journal of investigative dermatology.* 2014;134(2):366-73.
65. Kawasaki H, Isaacson T, Iwamuro S, and Conlon JM. A protein with antimicrobial activity in the skin of Schlegel's green tree frog Rhacophorus schlegelii (Rhacophoridae) identified as histone H2B. *Biochem Biophys Res Commun.* 2003;312(4):1082-6.
66. Hoeksema M, van Eijk M, Haagsman HP, and Hartshorn KL. Histones as mediators of host defense, inflammation and thrombosis. *Future Microbiol.* 2016;11(3):441-53.
67. Lee DY, Huang CM, Nakatsuji T, Thiboutot D, Kang SA, Monestier M, et al. Histone H4 is a major component of the antimicrobial action of human sebocytes. *J Invest Dermatol.* 2009;129(10):2489-96.
68. Acosta-Rodriguez EV, Rivino L, Geginat J, Jarrossay D, Gattorno M, Lanzavecchia A, et al. Surface phenotype and antigenic specificity of human interleukin 17-producing T helper memory cells. *Nat Immunol.* 2007;8(6):639-46.
69. Milner JD, Brenchley JM, Laurence A, Freeman AF, Hill BJ, Elias KM, et al. Impaired T(H)17 cell differentiation in subjects with autosomal dominant hyper-IgE syndrome. *Nature.* 2008;452(7188):773-6.
70. Happel KI, Dubin PJ, Zheng M, Ghilardi N, Lockhart C, Quinton LJ, et al. Divergent roles of IL-23 and IL-12 in host defense against Klebsiella pneumoniae. *The Journal of experimental medicine.* 2005;202(6):761-9.
71. Cho JS, Pietras EM, Garcia NC, Ramos RI, Farzam DM, Monroe HR, et al. IL-17 is essential for host defense against cutaneous Staphylococcus aureus infection in mice. *The Journal of clinical investigation.* 2010;120(5):1762-73.
72. Clark SR, Ma AC, Tavener SA, McDonald B, Goodarzi Z, Kelly MM, et al. Platelet TLR4 activates neutrophil extracellular traps to ensnare bacteria in septic blood. *Nat Med.* 2007;13(4):463-9.
73. Renner ED, Rylaarsdam S, Anover-Sombke S, Rack AL, Reichenbach J, Carey JC, et al. Novel signal transducer and activator of transcription 3 (STAT3) mutations, reduced T(H)17 cell numbers, and variably defective STAT3 phosphorylation in hyper-IgE syndrome. *The Journal of allergy and clinical immunology.* 2008;122(1):181-7.

74. Jiao H, Toth B, Erdos M, Fransson I, Rakoczi E, Balogh I, et al. Novel and recurrent STAT3 mutations in hyper-IgE syndrome patients from different ethnic groups. *Mol Immunol.* 2008;46(1):202-6.
75. Freeman AF, and Holland SM. The hyper-IgE syndromes. *Immunol Allergy Clin North Am.* 2008;28(2):277-91, viii.
76. Chen K, Eddens T, Trevejo-Nunez G, Way EE, Elsegeiny W, Ricks DM, et al. IL-17 Receptor Signaling in the Lung Epithelium Is Required for Mucosal Chemokine Gradients and Pulmonary Host Defense against K. pneumoniae. *Cell Host Microbe.* 2016;20(5):596-605.
77. Conti HR, Whibley N, Coleman BM, Garg AV, Jaycox JR, and Gaffen SL. Signaling through IL-17C/IL-17RE is dispensable for immunity to systemic, oral and cutaneous candidiasis. *PLoS One.* 2015;10(4):e0122807.
78. Lambert S, Hambro CA, Johnston A, Stuart PE, Tsoi LC, Nair RP, et al. Neutrophil Extracellular Traps Induce Human Th17 Cells: Effect of Psoriasis-Associated TRAF3IP2 Genotype. *J Invest Dermatol.* 2019;139(6):1245-53.
79. Uyemura K, Ohmen JD, Grisso CL, Sieling PA, Wyzykowski R, Reisinger DM, et al. Limited T-cell receptor beta-chain diversity of a T-helper cell type 1-like response to Mycobacterium leprae. *Infect Immun.* 1992;60(11):4542-8.
80. Schmidt NW, Agak GW, Deshayes S, Yu Y, Blacker A, Champer J, et al. Pentobra: A Potent Antibiotic with Multiple Layers of Selective Antimicrobial Mechanisms against Propionibacterium Acnes. *J Invest Dermatol.* 2015;135(6):1581-9.
81. McInturff JE, Wang SJ, Machleidt T, Lin TR, Oren A, Hertz CJ, et al. Granulysin-derived peptides demonstrate antimicrobial and anti-inflammatory effects against Propionibacterium acnes. *The Journal of investigative dermatology.* 2005;125(2):256-63.
82. Edgar R, Domrachev M, and Lash AE. Gene Expression Omnibus: NCBI gene expression and hybridization array data repository. *Nucleic Acids Res.* 2002;30(1):207-10.
83. Dobin A, Davis CA, Schlesinger F, Drenkow J, Zaleski C, Jha S, et al. STAR: ultrafast universal RNA-seq aligner. *Bioinformatics (Oxford, England).* 2013;29(1):15-21.
84. Robinson MD, and Oshlack A. A scaling normalization method for differential expression analysis of RNA-seq data. *Genome biology.* 2010;11(3):R25.

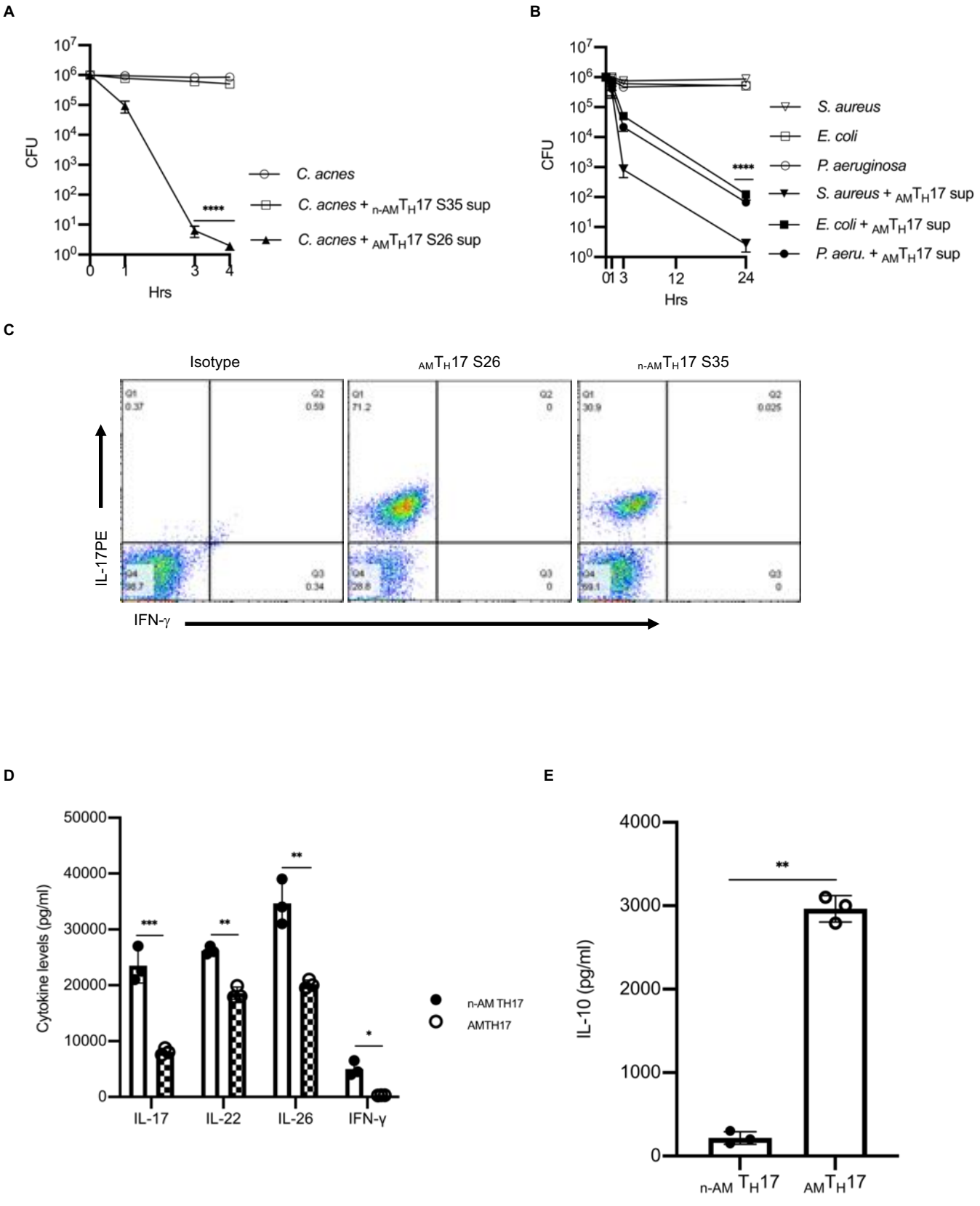

Fig. 1. $_{AM}T_H17$ secrete T_H17-associated cytokines and are antimicrobial against *C. acnes* and other bacterial strains. (A) Observed CFU activity against *C. acnes* strain HL005PA1 after 4 h incubation with $_{AM}T_H17$ clone S26 and $_{n\text{-}AM}T_H17$ clone S35 supernatants. (B) Observed CFU activity against several bacterial strains after 24 h incubation with $_{AM}T_H17$ clone S26 and $_{n\text{-}AM}T_H17$ clone S35 supernatants. Data represents the mean ± SEM. n>3. ****$p<0.0001$ by repeated measures 1-way ANOVA for treatment groups compared to $_{n\text{-}AM}T_H17$ supernatants in panel D and *C. acnes* in panel E. (C) $_{AM}T_H17$ and $_{n\text{-}AM}T_H17$ clones were stimulated with α-CD3/CD28 for 5h and IL-17 and IFN-γ expression determined by flow cytometry. n>3. (D-E) Cytokine levels in $_{AM}T_H17$ clones (S26, S27, S28) and $_{n\text{-}AM}T_H17$ clones (S35, S38, S44) as determined by ELISA. Data are shown as mean ± SEM. n>3 (D and E). *$p<0.05$, **$p<0.01$, **$p<0.001$ by 2-tailed Students's *t* test.

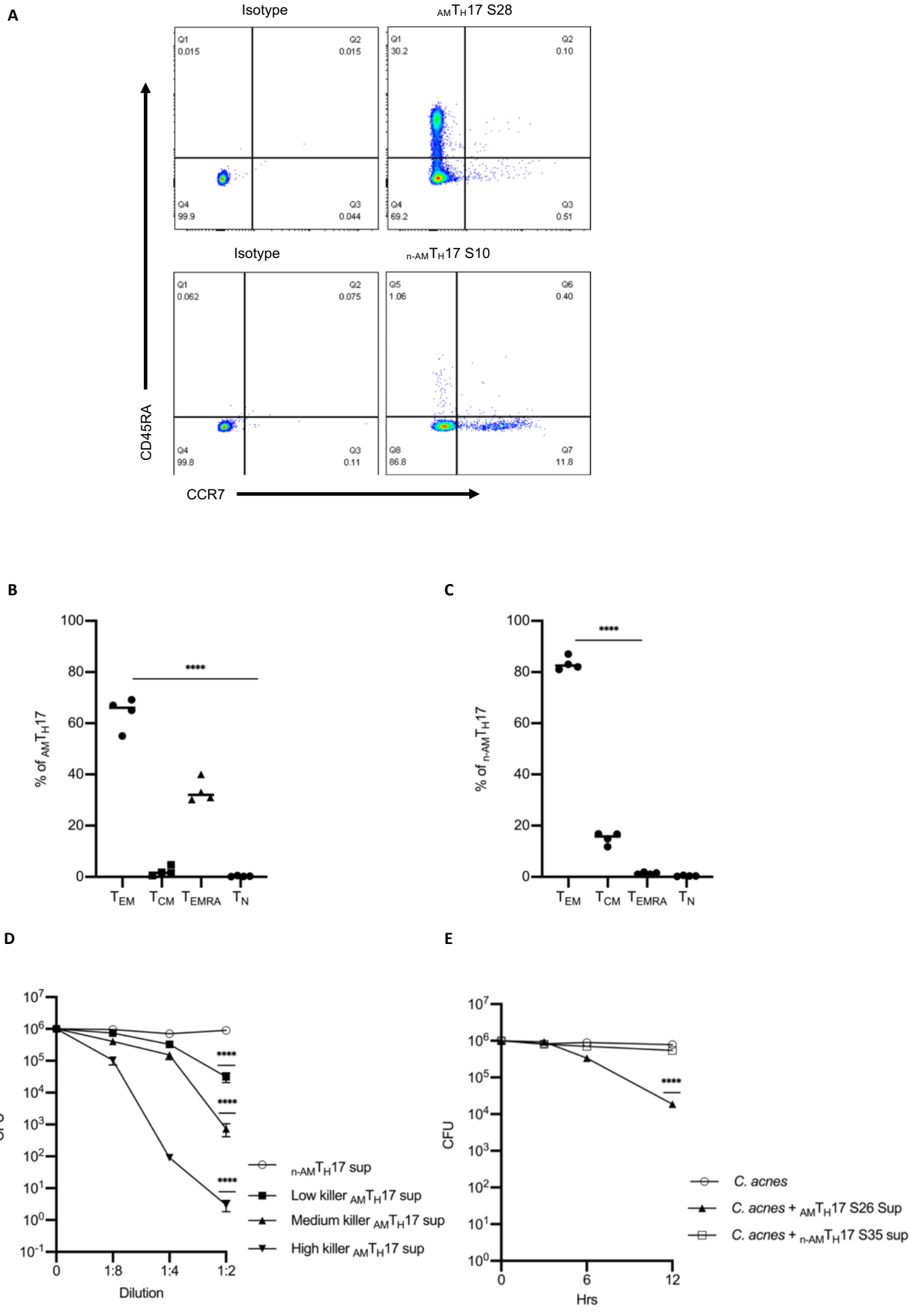

Fig. 2. $_{AM}T_H17$ are CD4$^+$ T_{EM} and T_{EMRA} cells and demonstrate antimicrobial activity as early as six hours. (A) $_{AM}T_H17$ and $_{n\text{-}AM}T_H17$ clones were stimulated with α-CD3/CD28 and stained with antibodies to CD4, CD45RA and CCR7. The $_{AM}T_H17$ clones consisted of primarily CD4$^+$CD45RA$^+$CCR7$^-$RA (T_{EM}) and CD4$^+$CD45RA$^-$CCR7$^-$ (T_{EMRA}) whereas the $_{n\text{-}AM}T_H17$ clones consisted mainly of T_{EM} and $^+$CD45RA$^-$CCR7$^+$ (T_{CM}). Data is representative of four independent experiments using clones derived from four different donors. (B and C) Analysis of memory markers in $_{AM}T_H17$ clones (S5, S16, S26, S28) and $_{n\text{-}AM}T_H17$ clones (S10, S13, S35, S38) by flow cytometry (n=4). ****$p<0.0001$ by repeated measures 1-way ANOVA for T_{EM} compared to T_{CM}, T_{EMRA} and T_N. (D) Several $_{AM}T_H17$ and $_{n\text{-}AM}T_H17$ clones were stimulated with α-CD3/CD28 and supernatants used for CFU assays against *C. acnes* strain HL096PA1. The $_{AM}T_H17$ clones were subsequently stratified into High, Medium, and Low based on the results of the CFU assays. ****$p<0.001$ by repeated measures 1-way ANOVA, Low, Medium and High killer $_{AM}T_H17$ compared to $_{n\text{-}AM}T_H17$. (E) Observed antimicrobial kinetics of supernatants derived from activated $_{AM}T_H17$ clones against several *C. acnes* strains (HL110PA1, HLA110PA3, HL043PA1, HL096PA1 HL005PA2, and ATCC6919) in CFU assays. Data are shown as mean ± SEM. n>3. ****$p<0.0001$ by repeated measures 1-way ANOVA for treatment groups compared to *C. acnes* control.

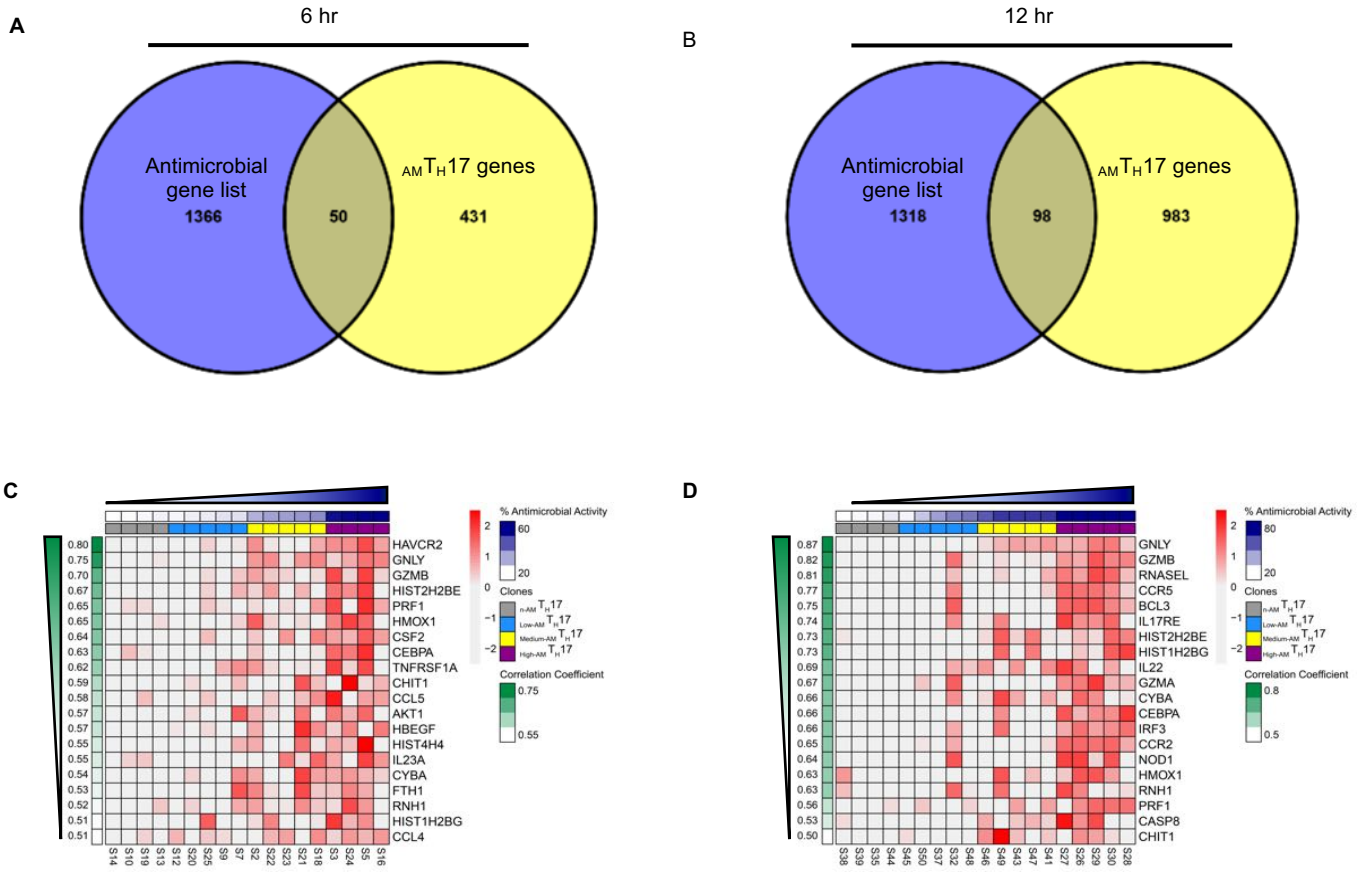

Fig. 3. Antimicrobial transcripts are highly expressed in $_{AM}T_H17$. (A and B) $_{AM}T_H17$ genes with a log_2Fold-change (FC) >2 and positively correlated with % antimicrobial activity (r>0.5) were overlapped with an antimicrobial gene list from the Gene Cards database. (C-D) Heatmap of the top 20 highest correlated genes with % antimicrobial activity found in the $_{AM}T_H17$ clones with Low (sky blue), Medium (yellow) and High (purple) antimicrobial activity against *C. acnes* at 6h (C) and 12h (D). Annotation for % antimicrobial activity and correlation coefficient values for each sample and gene are displayed on top (dark blue) and on the left (green). Gene expression values are displayed as Z-scores of log_{10} normalized counts.

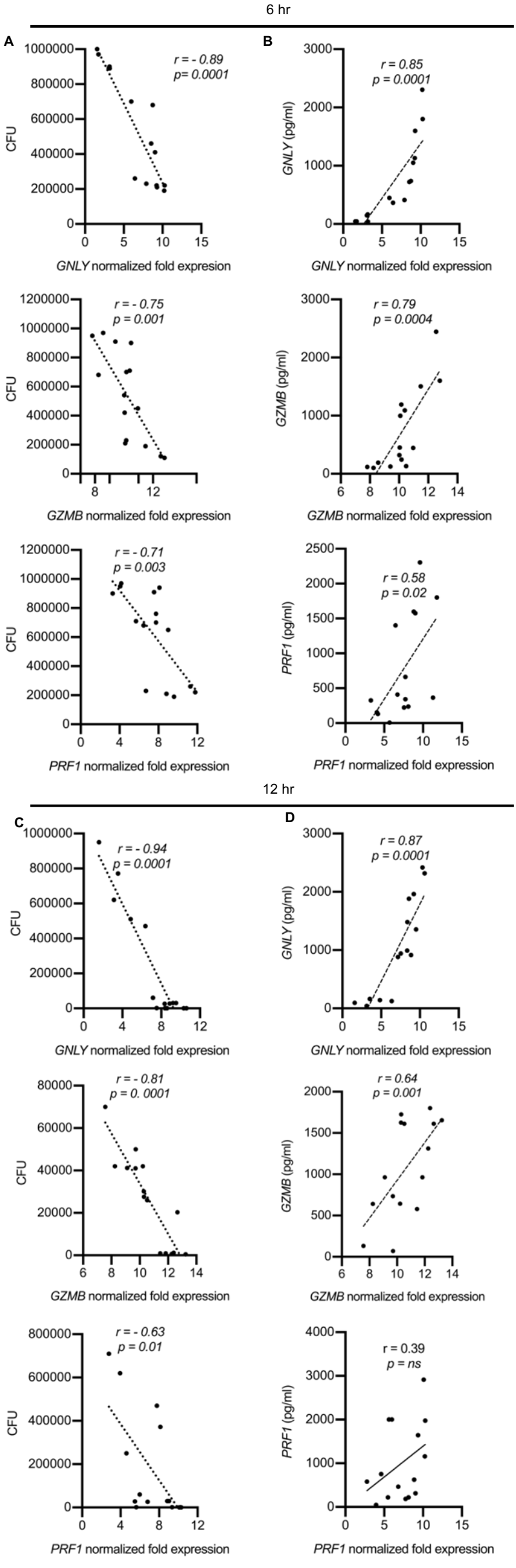

Fig. 4. Antimicrobial gene expression in $_{AM}T_H17$ clones highly correlate with both protein secretion and antimicrobial CFU activity. (A-D) Correlation plots of *GNLY, PRF1* and *GZMB* expression in stimulated $_{AM}T_H17$ as determined by RNA-seq. Specific $_{AM}T_H17$ gene signatures with a twofold or more expression in comparison to the $_{n\text{-}AM}T_H17$ clones and that highly correlated with *C. acnes* CFU activity (A and C) and ELISA protein secretion (B and D) are shown for the 6h and 12h time points. *p* value by Student's *t* test (n=15).

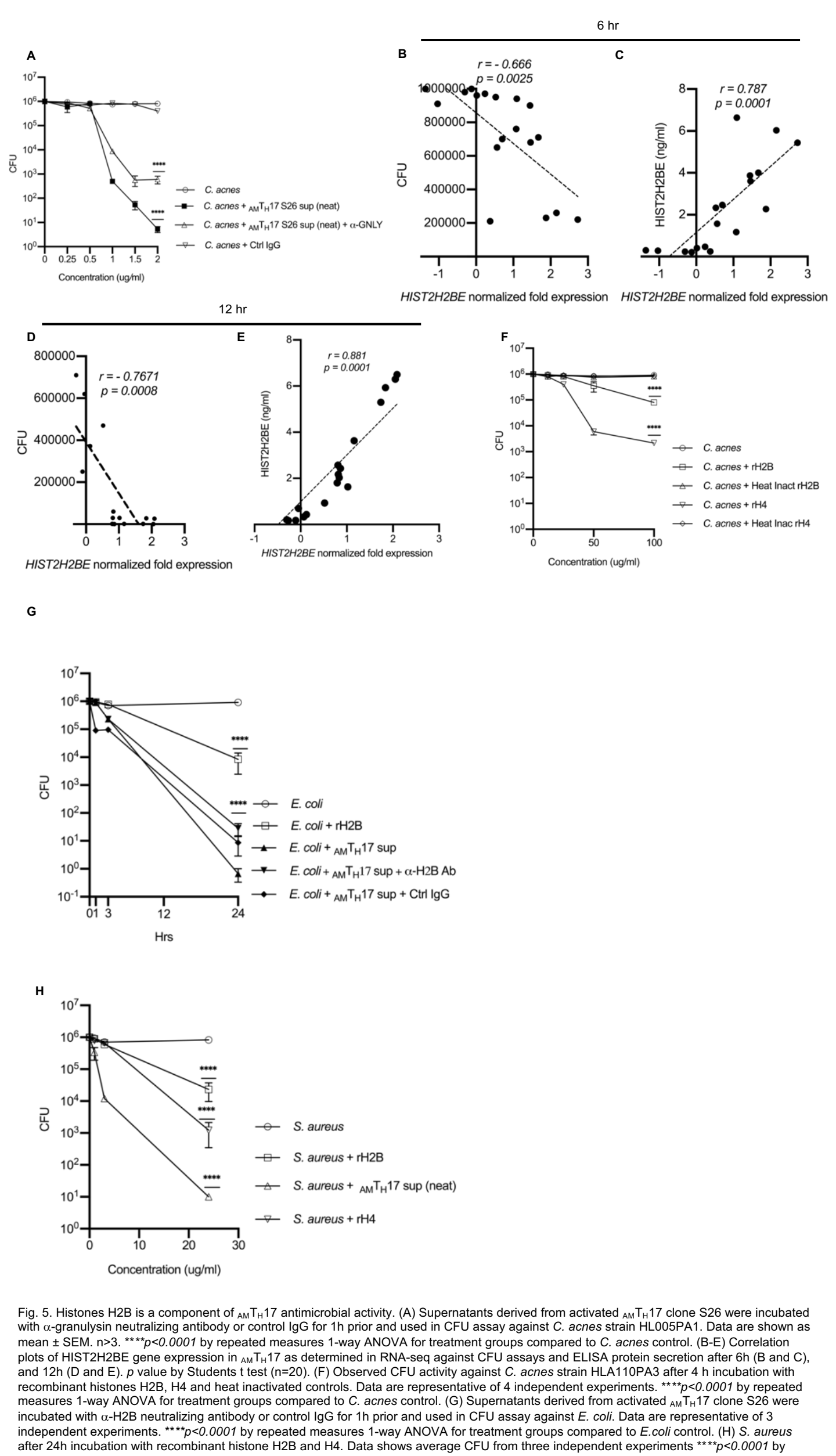

Fig. 5. Histones H2B is a component of $_{AM}T_H17$ antimicrobial activity. (A) Supernatants derived from activated $_{AM}T_H17$ clone S26 were incubated with α-granulysin neutralizing antibody or control IgG for 1h prior and used in CFU assay against *C. acnes* strain HL005PA1. Data are shown as mean ± SEM. n>3. ****$p<0.0001$* by repeated measures 1-way ANOVA for treatment groups compared to *C. acnes* control. (B-E) Correlation plots of HIST2H2BE gene expression in $_{AM}T_H17$ as determined in RNA-seq against CFU assays and ELISA protein secretion after 6h (B and C), and 12h (D and E). *p* value by Students t test (n=20). (F) Observed CFU activity against *C. acnes* strain HLA110PA3 after 4 h incubation with recombinant histones H2B, H4 and heat inactivated controls. Data are representative of 4 independent experiments. ****$p<0.0001$* by repeated measures 1-way ANOVA for treatment groups compared to *C. acnes* control. (G) Supernatants derived from activated $_{AM}T_H17$ clone S26 were incubated with α-H2B neutralizing antibody or control IgG for 1h prior and used in CFU assay against *E. coli*. Data are representative of 3 independent experiments. ****$p<0.0001$* by repeated measures 1-way ANOVA for treatment groups compared to *E.coli* control. (H) *S. aureus* after 24h incubation with recombinant histone H2B and H4. Data shows average CFU from three independent experiments ****$p<0.0001$* by repeated measures 1-way ANOVA for treatment groups compared to *S. aureus* control.

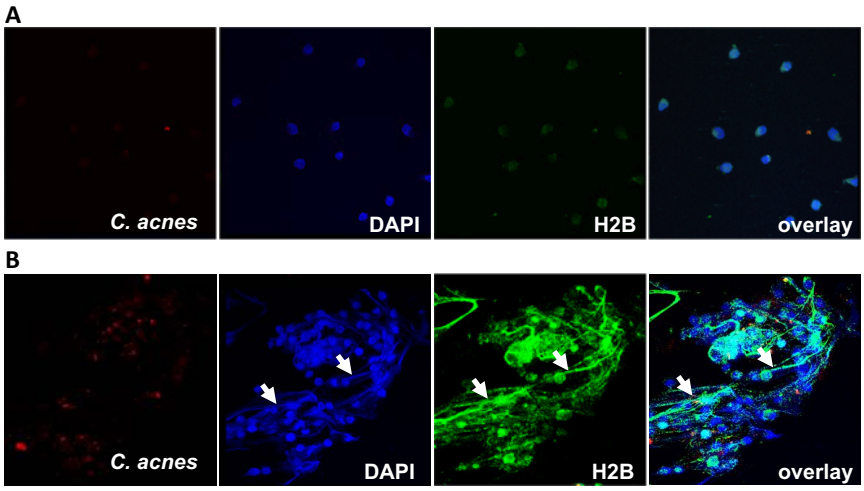

Fig. 6. $_{AM}T_H17$ extracellular structures are prominently coated with Histone H2B. (A-B) $_{n\text{-}AM}T_H17$ clones S13 (A) and $_{AM}T_H17$ clone S16 (B) were stimulated with PMA for 2 hours as previously described (*42*) and incubated with PKH-labeled *C. acnes* (red) (1:1). Cells were fixed, and stained with DAPI (blue) and α-histone H2B (green). Confocal staining images are shown. White arrows indicate T cell extracellular traps and ensnared *C. acnes.* Magnification 63X.

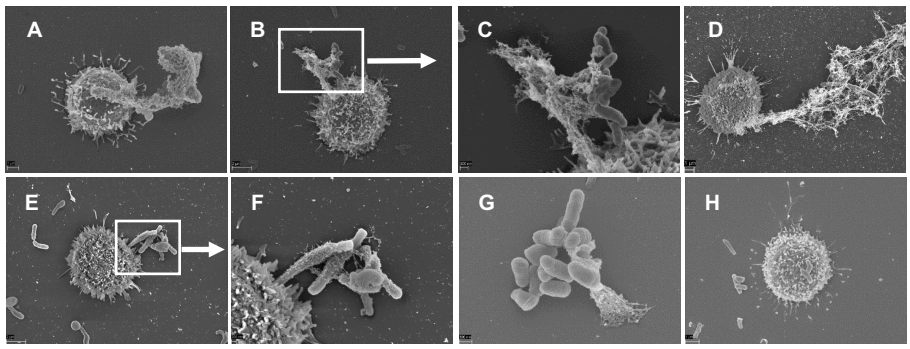

Fig. 7. Antimicrobial T_H17 release extracellular traps that entangle *C. acnes.* Scanning electron microscopy of the interaction of $_{AM}T_H17$ and *C. acnes* at different time points. (A) $_{AM}T_H17$ clones were stimulated with PMA for 30 minutes. (B and C) PMA and *C. acnes* for 30 minutes. (D) α-CD3/CD28 for 30 minutes. (E and F) *C. acnes* 30 minutes. (G) PMA and *C. acnes* for 40 minutes, and (H) PMA, *C. acnes* and DNase for 40 minutes (*42*). Extended and released TETs can be seen attached to bacteria.

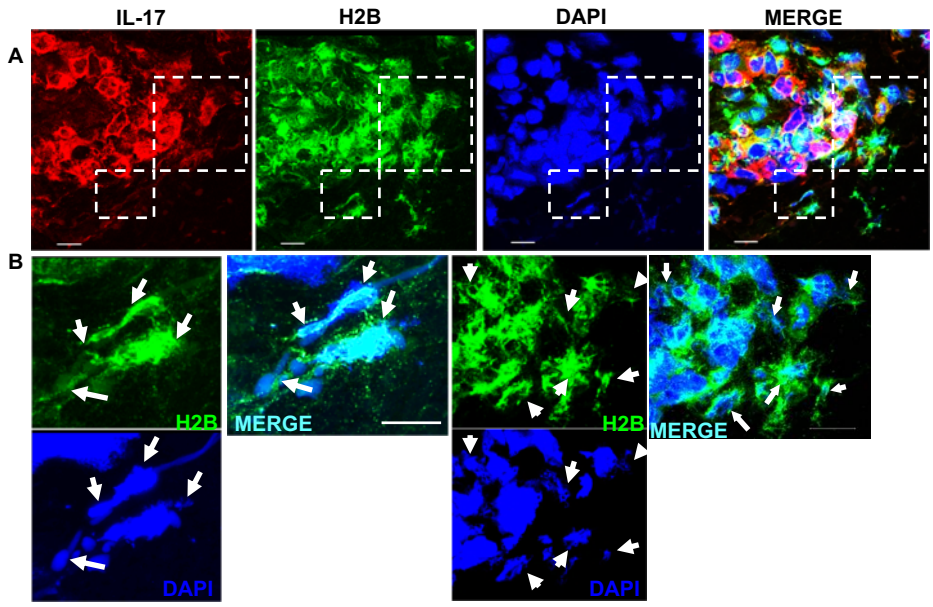

Fig. 8 Expression of T cell extracellular traps in acne lesions. (A). Confocal images of IL-17 (red), histone H2B (green), and nuclei (DAPI, blue) in acne lesions. Dashed-line boxes identify the area further studied at higher power. (B). Higher power magnification of the delineated regions marked in (A) showing H2B (green) and DAPI (red) only. White arrows indicate T cell extracellular traps in proximity to $CD4^{+}IL\text{-}17^{+}H2B^{+}$ triple-positive cells within acne lesions. TETs are visualized as fibrous structures containing DNA (DAPI, blue) decorated with histone H2B (green) in the extracellular space. The images are projections of confocal z stacks generated from sections of 10μm thickness. Magnification, (A) 63X with zoom 2X from lower magnification in supplemental figure S9, and (B) is zoom 4X from (A). Data is from three individual samples. Scale bar, 10μm (enlarged insets).

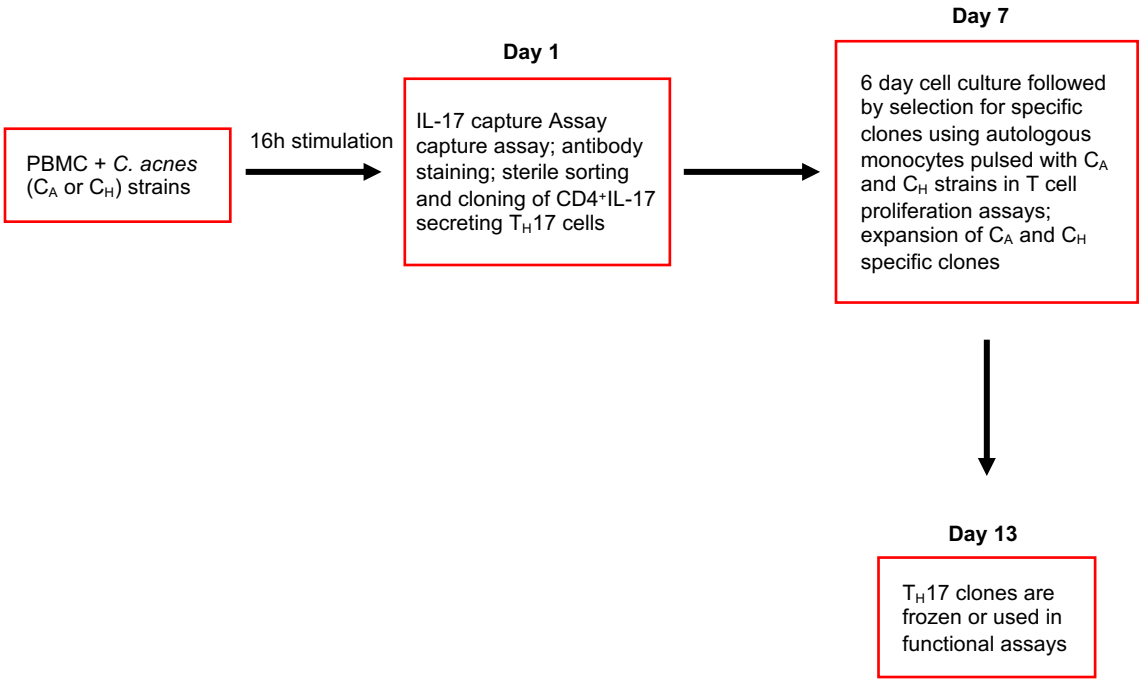

Fig. S1. Scheme for generation of T_H17 clones. PBMCs were isolated from normal donors and stimulated for 16 hours with either C_H or C_A associated *C. acnes* strains. Cytokine secretion was determined using IL-17 cytokine secretion capture assay. After IL-17 staining, cells were further stained with α-CD4 antibodies and the $CD4^+$ $IL\text{-}17^+$ cells sorted under sterile conditions and cloned in Terasaki plates. On day 7, *C. acnes*-specific clones were selected using T cell proliferation assays (*30*) followed by a further 6-day expansion in 24 well plates in T cell media supplemented with 100 U/ml IL-2 and 2ng/ml IL-23. On day 13, T_H17 cell clones were either frozen, and/or used immediately in subsequent functional experiments.

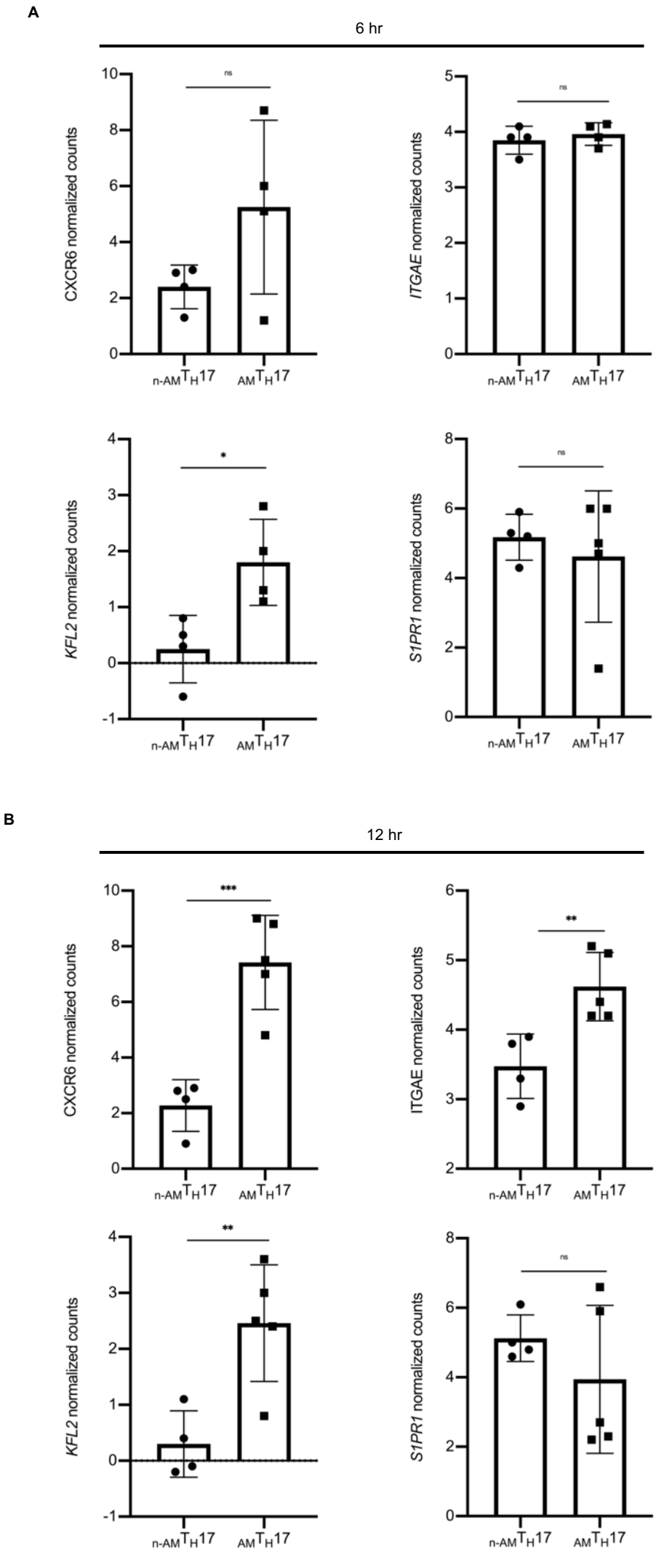

Fig. S2. Tissue resident memory T cell markers expressed by T_H17 clones. (A and B). Normalized count expression of tissue resident memory T cell genes, *CXCR6, ITGAE (CD103), KFL2* and *S1PR1* expression in $_{AM}T_H17$ compared to $_{n\text{-}AM}T_H17$ clones as determined by RNA-seq after 6h (A) and 12h (B) stimulation with α-CD3/CD28 antibodies are shown. *$p<0.05$, **$p<0.01$, ***$p<0.001$ by 2-tailed Students's *t* test.

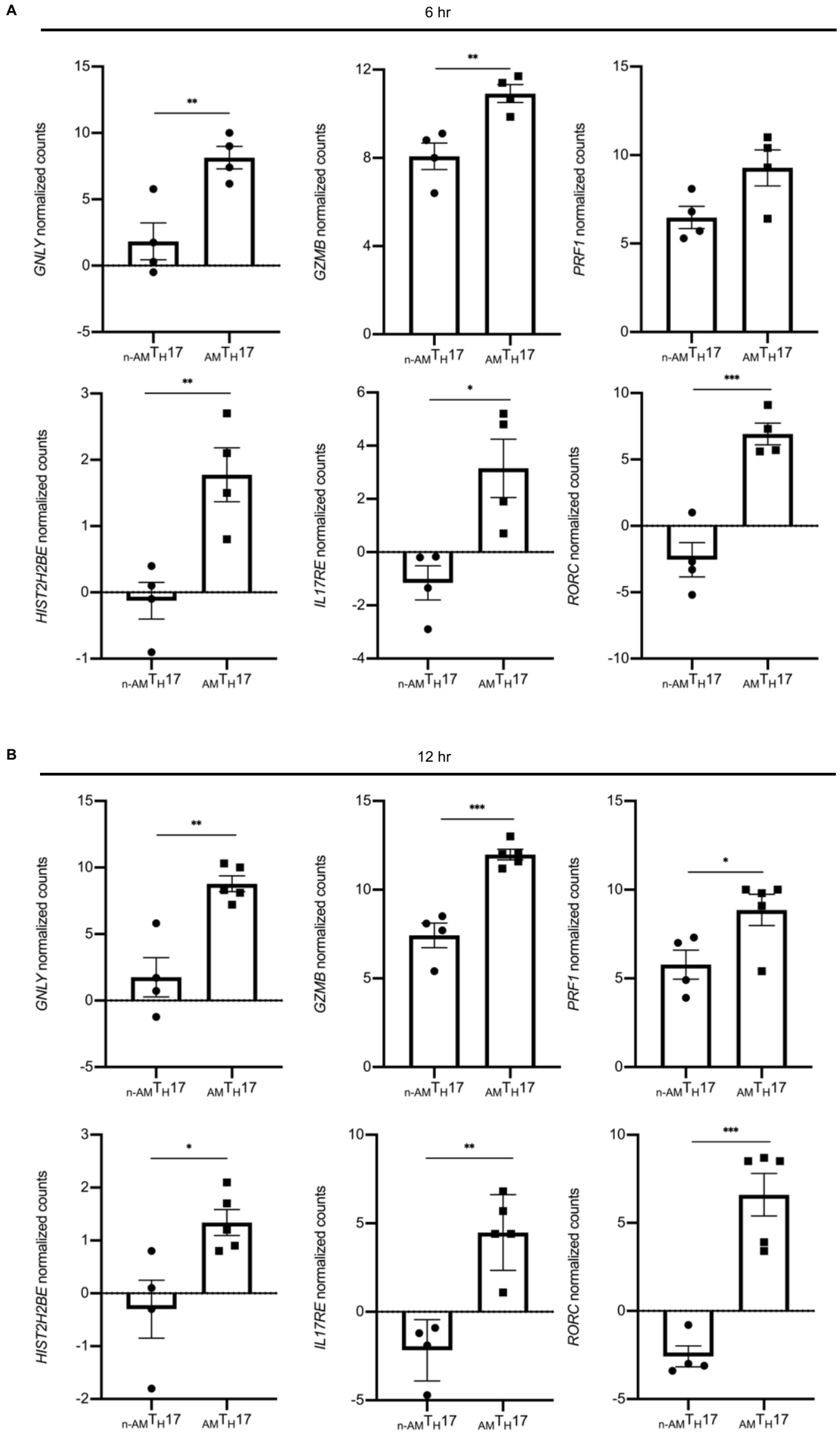

Fig. S3. $_{AM}T_H17$ antimicrobial signatures revealed by RNA-seq. (A and B). Normalized count expression of antimicrobial-related genes, transcriptional factors, and IL17-associated receptor genes in $_{AM}T_H17$ compared to $_{n\text{-}AM}T_H17$ clones as determined by RNA-seq after 6h (A) and 12h (B) stimulation with α-CD3/CD28 antibodies are shown. *$p<0.05$, **$p<0.01$, ***$p<0.001$ by 2-tailed Students's *t* test.

A

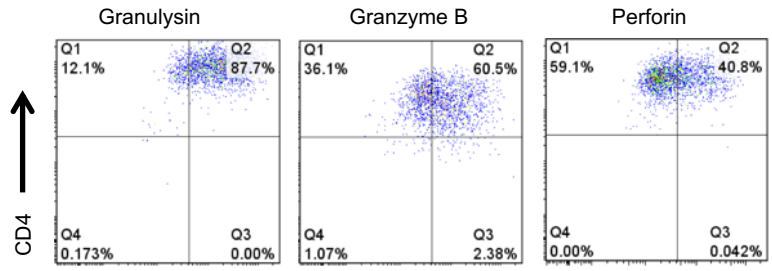

B

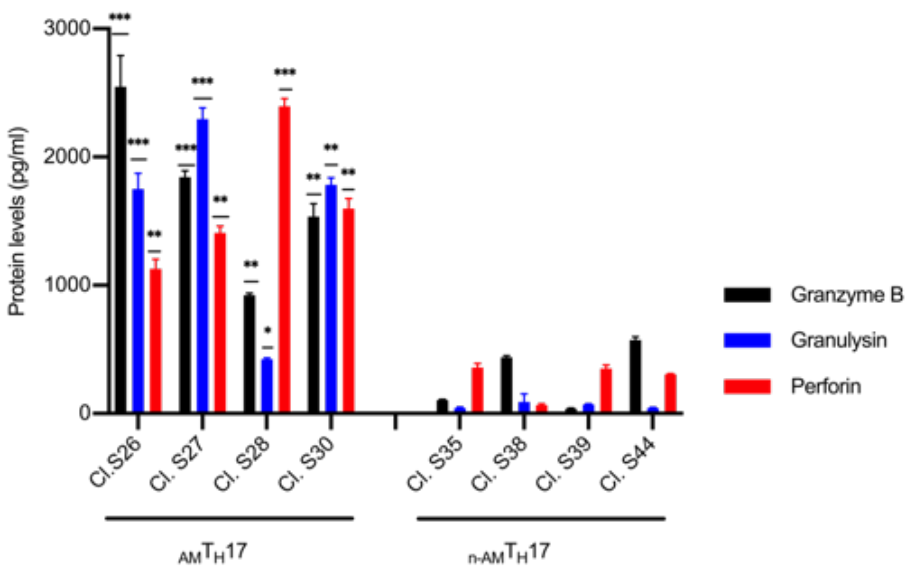

Fig. S4. Secretion of antimicrobial molecules by $_{AM}T_H17$ (A) Flow cytometry of a representative $_{AM}T_H17$ clone S26 stimulated with α-CD3/CD28 antibodies and stained for granulysin, granzyme B and perforin. Data is representative of three independent experiments. (B) Secretion of cytotoxic molecules by $_{AM}T_H17$ compared to $_{n\text{-}AM}T_H17$ clones as measured by ELISA. *$p<0.05$, **$p<0.01$, ***$p<0.001$ by 2-tailed Students's *t* test.

A

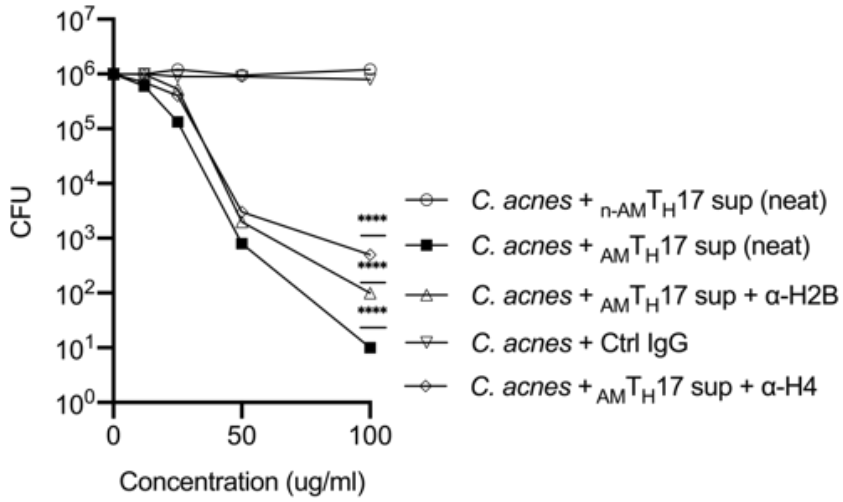

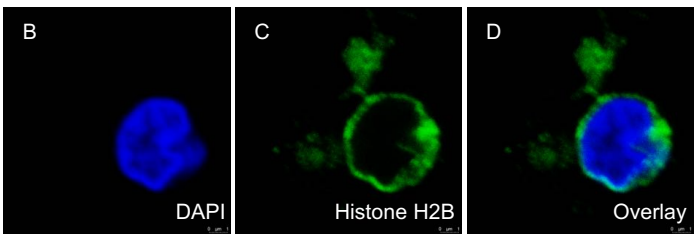

Fig. S5. Effects of neutralizing histone H2 and H4 on $_{AM}T_H17$ antimicrobial activity. (A) Supernatants derived from activated $_{AM}T_H17$ and $_{n\text{-}AM}T_H17$ clones were incubated with α-H2B and α-H4 neutralizing antibodies for 1h and used for CFU assay against *C. acnes* strain HL005PA1. Data is representative of three independent experiments. ****$p<0.0001$ by repeated measures 1-way ANOVA for treatment groups compared to *C. acnes* + $_{n\text{-}AM}T_H17$ control. (B-D) Confocal microscopy of $_{AM}T_H17$ clone S26 stimulated with PMA for 30 minutes, fixed, and stained with (B) DAPI (blue) (C) Histone H2B (green) (D) an overlay of DAPI and Histone H2B. Original magnification: ×63.

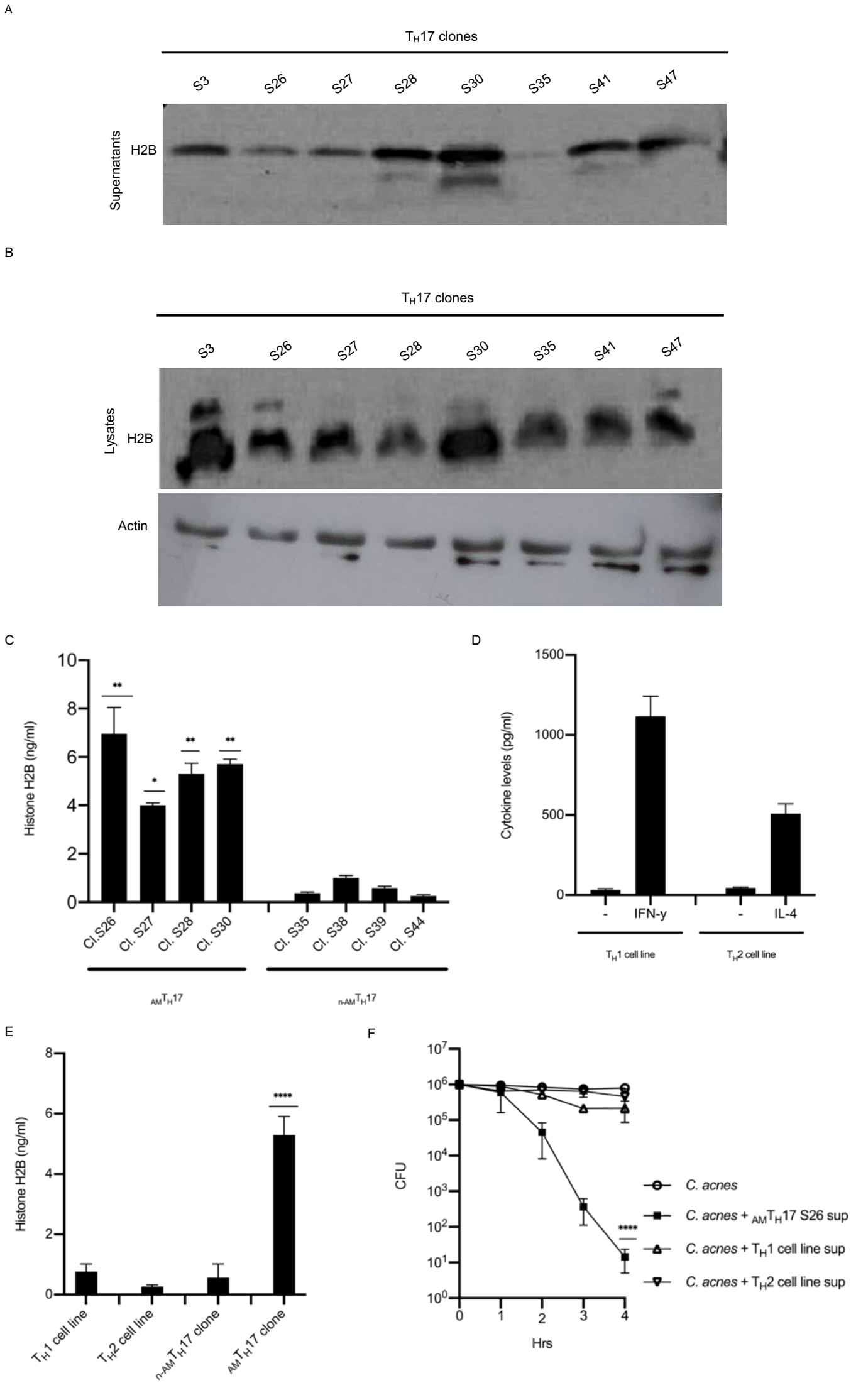

Fig. S6. Histones H2B expression in $_{AM}T_H17$ clones. Western blotting analysis of histone H2B protein expression in (A) supernatants and (B) lysates derived from activated $_{AM}T_H17$ and $_{n\text{-}AM}T_H17$ clones. (C) Secretion of histone H2B by $_{AM}T_H17$ compared to $_{n\text{-}AM}T_H17$ clones as measured by ELISA. ****$p<0.0001$ by repeated measures 1-way ANOVA for $_{AM}T_H17$ supernatants compared to $_{n\text{-}AM}T_H17$ Cl. S38 control. (D and E) Secretion of IFN-γ, IL-4 and histone H2B by T_H1 and T_H2 cell lines as measured by ELISA. ****$p<0.001$ by repeated measures 1-way ANOVA for $_{AM}T_H17$ clone compared to T_H1 cell line. (F) Several T_H1 and T_H2 cell lines were stimulated with PMA and supernatants used for CFU assays against *C. acnes* strain HL096PA1. Observed CFU activity is shown. ****$p<0.001$ by repeated measures 1-way ANOVA for $_{AM}T_H17$ S26 clone compared to a T_H2 cell line.

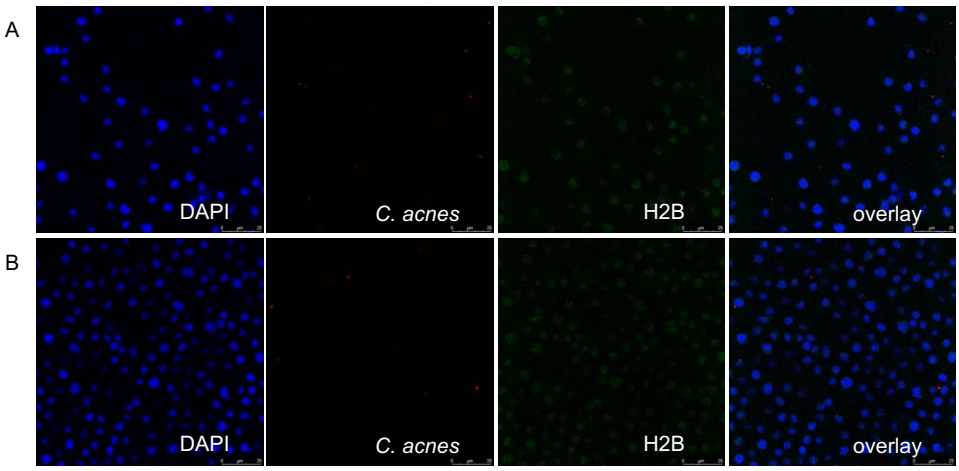

Fig. S7. Characterization of histone H2B expression on T_H1 and T_H2 cell lines. (A-B) T_H1 (A) and T_H2 cell line (B) were stimulated with PMA for 2 hours as previously described and incubated with PKH-labeled *C. acnes* (red) (1:1). Cells were fixed, stained with DAPI (blue) and α-histone H2B isotype control antibodies (green). Confocal staining images are shown. Original magnification: x63.

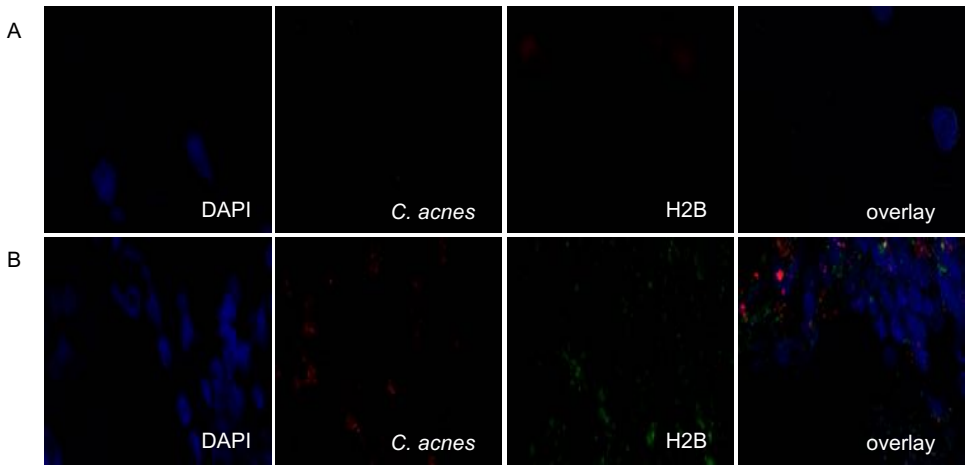

Fig. S8. $_{AM}T_H17$ extracellular structures are prominently coated with Histone H2B. (A-B) $_{n\text{-}AM}T_H17$ clone S13 (A) and $_{AM}T_H17$ clone S16 (B) were stimulated with PMA for 2 hours as previously described (*42*) and incubated with PKH-labeled *C. acnes* (red) (1:1). Cells were fixed, stained with DAPI (blue) and α-histone H2B isotype control antibodies (green). Confocal staining images are shown. Original magnification: x63.

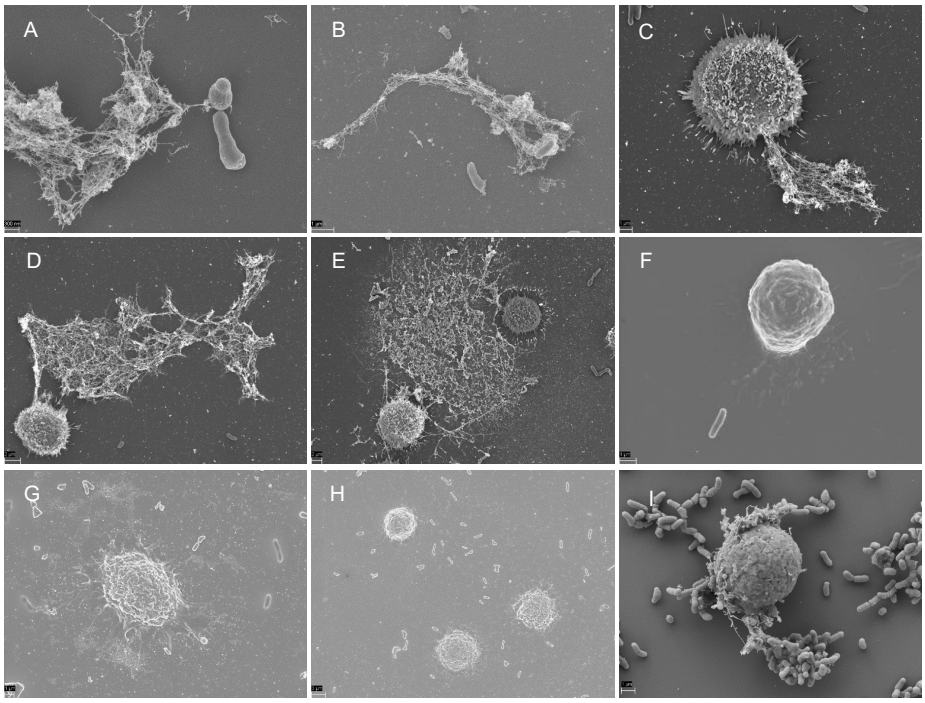

Fig. S9. $_{AM}T_H17$ release extracellular traps that entangle *C. acnes.* Scanning electron microscopy of the interaction of $_{AM}T_H17$ and $_{n\text{-}AM}T_H17$ clones with *C. acnes* at different time points. (A-B) $_{AM}T_H17$ clones were stimulated with PMA and *C. acnes* for 60 minutes. (C-E) $_{AM}T_H17$ clones stimulated with α-CD3/CD28 antibodies for 20, 30 and 60 minutes respectively. (F) $_{n\text{-}AM}T_H17$ clone stimulated with PMA and *C. acnes* 30 minutes. (G) $_{n\text{-}AM}T_H17$ clone stimulated with PMA and *C. acnes* + DNase 90 minutes. (H) $_{AM}T_H17$ clone stimulated with PMA and *C. acnes* + DNase 90 minutes. (I) neutrophil stimulated for 30 minutes with PMA and *C. acnes* positive control (*42*).

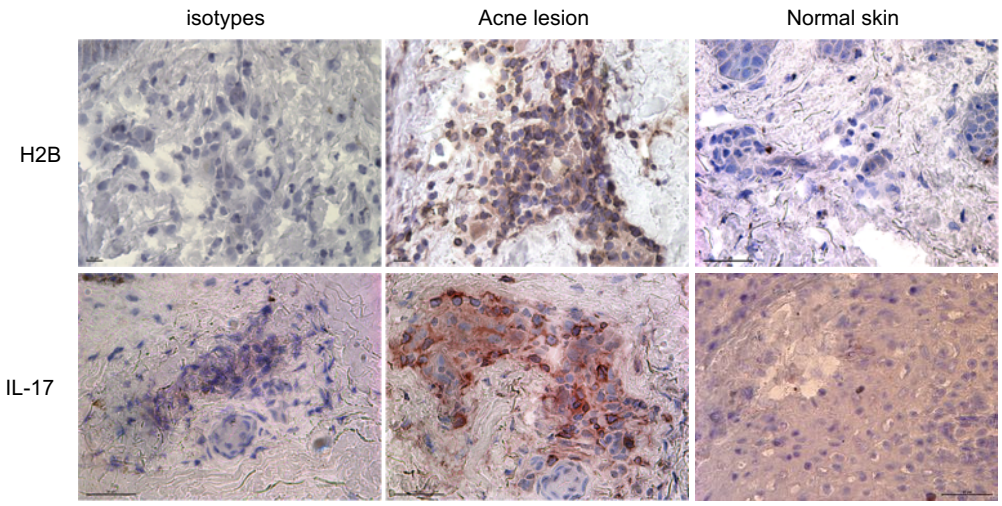

Fig. S10 Histone H2B and IL-17 expression in acne lesions. Representative section from skin biopsy specimens of normal and acne lesions stained by the immunoperoxidase method with monoclonal antibodies specific for histone H2B, IL-17 and corresponding isotype controls (n=3). Multiple histone H2B and IL-17-positive cells (brown) can be seen scattered around the dermis. Original magnification: x40.

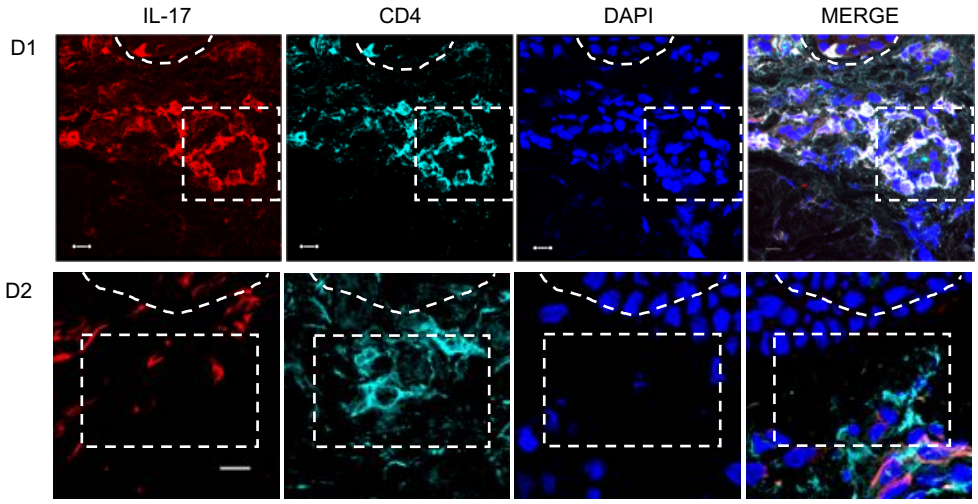

Fig. S11. Colocalization of $CD4^+IL\text{-}17^+$ T cells in acne lesions. High power confocal images of IL-17 (red), CD4 (cyan), and nuclei (DAPI, blue) in acne lesions of two donors (D1 and D2). Merge indicate $CD4^+$T cell secreting IL-17 within acne lesions. Dashed-line boxes identify the area further studied at higher power. The images are projections of confocal z stacks generated from sections of 10μm thickness. Scale bar, 10μm (enlarged insets). Original magnification: ×63.

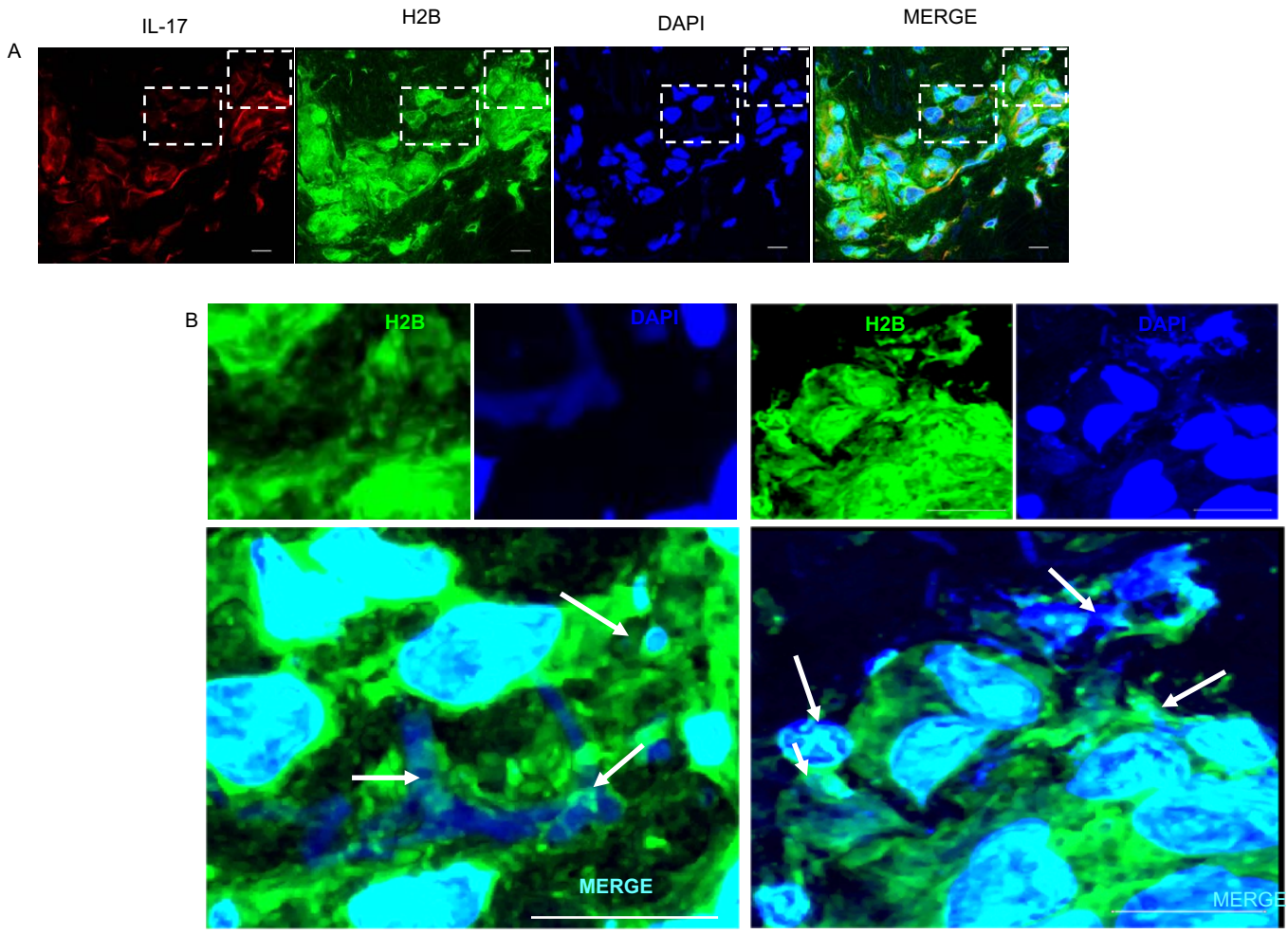

Fig. S12. Colocalization of IL-17^{+}H2B^{+} T cells in acne lesions. (A) Confocal images of IL-17 (red), histone H2B (green), and nuclei (DAPI, blue) in acne lesions. Dashed-line boxes identify the area further studied at higher power. (B). Higher power magnification of the delineated regions marked in (A) showing H2B (green) and DAPI (blue) only. White arrows indicate T cell extracellular traps in proximity to CD4^{+}IL-17^{+}H2B^{+} triple-positive cells within acne lesions. TETs are visualized as fibrous structures containing DNA (DAPI, blue) decorated with histone H2B (green) in the extracellular space. The images are projections of confocal z stacks generated from sections of 10μm thickness. Magnification, (A) 63X with zoom 2X from lower magnification in supplemental figure S11, and (B) is zoom 4X from (A). Data is from three individual samples. Scale bar, 10μm (enlarged insets).

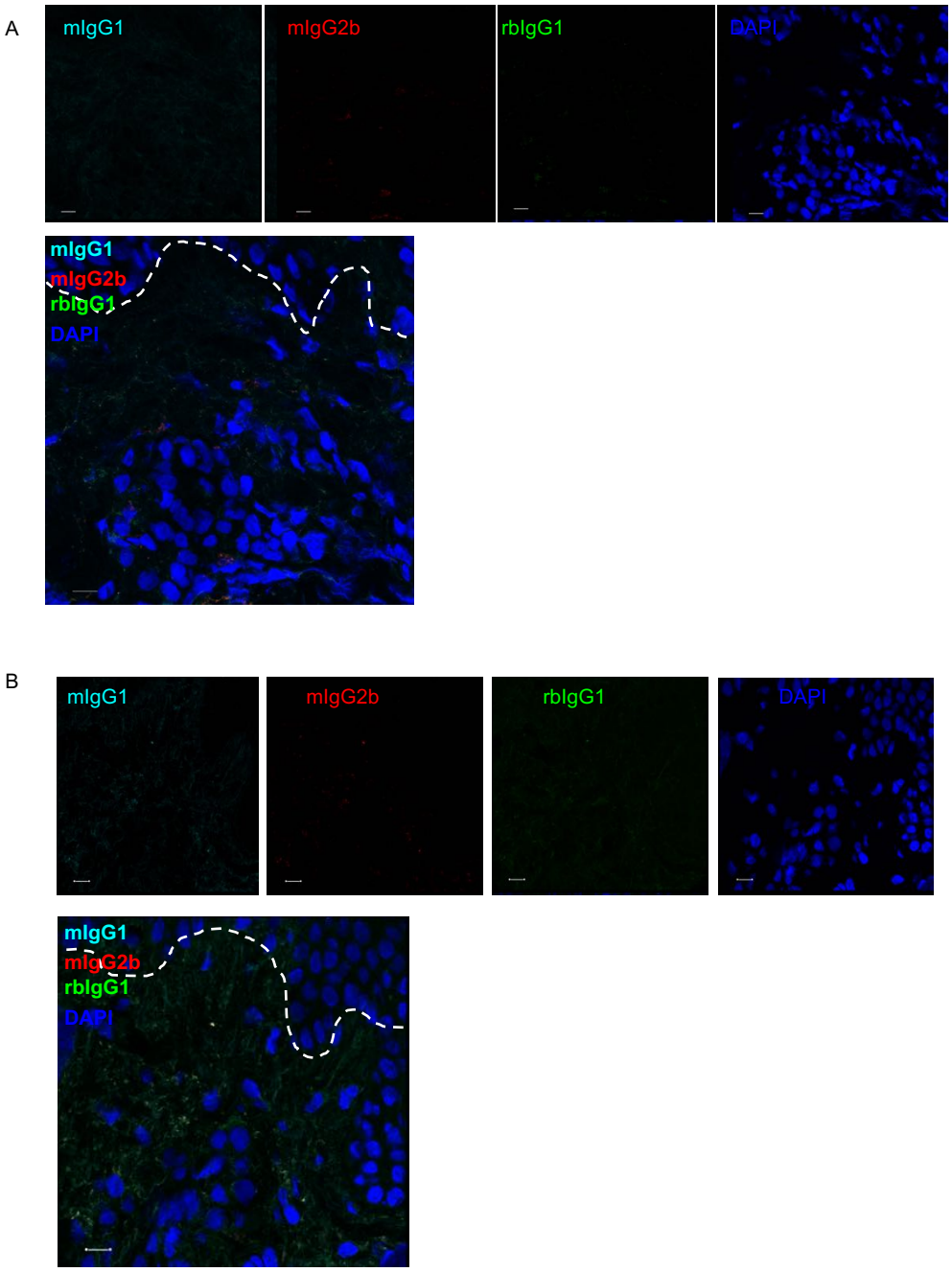

Fig. S13. Colocalization of IL-17^{+}H2B^{+} T cells in acne lesions. (A) High power confocal images of acne lesions from donor D1 labeled with isotype control antibodies; CD4 isotype (mIgG1; cyan), IL-17 isotype (mIgG2b; red), histone H2B isotype (rabbit IgG; green), and nuclei (DAPI, blue). (B) High power confocal images of acne lesions from donor D2 labeled with isotype control antibodies; CD4 isotype (mIgG1; cyan), IL-17 isotype (mIgG2b; red), histone H2B isotype (rabbit IgG; green), and nuclei (DAPI, blue). The images are projections of confocal z stacks generated from sections of 10μm thickness. Scale bar, 10μm (enlarged insets). Original magnification: ×63.

EXOC8	HDAC9	AQP3
ITGAM	CCND1	LGALS1
ATN1	CCR1	PROCR
SRC	EGLN2	PLEK
HSPA1B	ABCC1	ZBP1
CSF1	GJB2	TRIM8
ACO1	TNFRSF1B	SPSB2
IL17RE	SIK2	F3
BIRC3	TGIF1	CTSB
SMAD7	PXN	SETBP1

Table S1. Common genes expressed in the $_{AM}T_H17$ clones after 6h stimulation. Specific $_{AM}T_H17$ gene signatures with a twofold or more expression in comparison to the $_{n\text{-}AM}T_H17$ clones and that highly correlated with CFU activity were overlapped with an antimicrobial gene list from the Gene Cards database. 30 common genes at 6h time point are listed. The top 20 genes are listed in figure 3.

CCL1	BAX	CCR1	SP1	CASP4	SYTL1
F2R	FTL	EGLN2	ALOX5AP	AQP3	PELI3
CSF2	ACO1	USF1	HAVCR2	SLC22A4	SPSB2
HBEGF	AKT1	MYBL1	FPGS	RELB	
PLA2G2C	HLA-DRB1	LYPD3	MAP2K2	PYCARD	
CXCR3	TNFRSF1A	CHP1	PLCD1	LGALS1	
FTH1	SMAD7	CEBPB	PLD2	GDI1	
RHOA	NEO1	TYK2	VAV1	TNFRSF18	
NR1H2	HDAC9	IFNGR1	PINK1	SH3KBP1	
MAP3K3	BAK1	CASP9	GGT1	SETBP1	
FURIN	IL2RB	PLD1	PAK1	PLEK	
CFH	HLA-DRB5	CDKN1A	SERPINH1	SECTM1	
ITGB2	VHL	CTSB	ANXA2	BHLHE40	
CRAT	ITGA3	TNFRSF1B	TGIF1	ZBP1	
ULK1	GALE	ERN1	PXN	TRIM8	

Table S2. Common genes expressed in the $_{AM}T_H17$ clones after 12h stimulation. Specific $_{AM}T_H17$ gene signatures with a twofold or more expression in comparison to the $_{N\ n\text{-}AM}T_H17$ clones and that highly correlated with CFU activity were overlapped with an antimicrobial gene list from the Gene Cards database. 78 common genes at the 12h time point are listed. The top 20 genes are listed in figure 3.

MERGE